NASA HERMeS Hall Thruster Electrical Configuration Characterization

Peter Y. Peterson[1]
Vantage Partners, LLC
NASA Glenn Research Center, Cleveland, OH, 44135

Hani Kamhawi[2], Wensheng Huang[3], John Yim[4], and Daniel Herman[5]
NASA Glenn Research Center, Cleveland, OH, 44135

George Williams[6], and James Gilland[7]
Ohio Aerospace Institute
NASA Glenn Research Center, Cleveland, OH, 44135

and

Richard Hofer[8],
Jet Propulsion Laboratory, California Institute of Technology, Pasadena, CA, 91109

The NASA Hall Effect Rocket with Magnetic Shielding (HERMeS) 12.5 kW Technology Demonstration Unit-1 (TDU-1) Hall thruster has been the subject of extensive technology maturation in preparation for development into a flight ready propulsion system. Part of the technology maturation was to test the TDU-1 thruster in several ground based electrical configurations to assess the thruster robustness and suitability to successful in-space operation. The ground based electrical configuration testing has recently been demonstrated as an important step in understanding and assessing how a Hall thruster may operate differently in-space compared to ground based testing, and to determine the best configuration to conduct development and qualification testing. This paper describes the electrical configuration testing of the HERMeS TDU-1 Hall thruster in NASA Glenn Research Center's Vacuum Facility 5. The three electrical configurations examined were 1) thruster body tied to facility ground, 2) thruster floating, and 3) thruster body electrically tied to cathode common. The HERMeS TDU-1 Hall thruster was also configured with two different exit plane boundary conditions, dielectric and conducting, to examine the influence on the electrical configuration characterization.

I. Introduction

For missions beyond low Earth orbit, spacecraft size and mass can be dominated by onboard chemical propulsion systems and propellants that may constitute more than 50 percent of the spacecraft mass. This impact can be substantially reduced through the utilization of Solar Electric Propulsion (SEP) due to its substantially higher specific impulse. Studies performed for NASA's Human Exploration and Operations Mission Directorate and Science Mission Directorate have demonstrated that a 50kW-class SEP capability can be enabling for both near term and future

[1] Senior Research Engineer, Electric Propulsion Systems Branch, peter.y.peterson@nasa.gov, AIAA Senior Member.
[2] Senior Research Engineer, Electric Propulsion Systems Branch, hani.kamhawi-1@nasa.gov AIAA Associate Fellow.
[3] Research Engineer, Electric Propulsion Systems Branch, wensheng.huang@nasa.gov, AIAA Senior Member.
[4] Research Engineer, Electric Propulsion Systems Branch, john.t.yim@nasa.gov, AIAA Member.
[5] Research Engineer, Electric Propulsion Systems Branch, daniel.a.herman@nasa.gov, AIAA Senior Member.
[6] Principle Scientist, Electric Propulsion Systems Branch, george.j.williams@nasa.gov, AIAA Associate Fellow.
[7] Research Team Manager, Electric Propulsion Systems Branch, james.h.gilland@nasa.gov, AIAA Associate Fellow.
[8] Senior Engineer, Electric Propulsion Group, richard.r.hofer@ nasa.gov, AIAA Associate Fellow.

architectures and science missions [1]. To enable SEP missions at the power levels required for these applications, an in-space demonstration of an operational 50kW-class SEP spacecraft has been proposed as an SEP Technology Demonstration Mission (TDM). In 2010 NASA's Space Technology Mission Directorate (STMD) began developing large, deployable photovoltaic solar array structures for high-power electrical power production and high-power electric propulsion technologies [2-7]. The maturation of these critical technologies has made mission concepts utilizing high-power SEP viable.

The Asteroid Redirect Robotic Mission (ARRM) is the leading candidate for the SEP TDM concepts that utilizes an SEP spacecraft to return up to 20 metric tons (up to 6 m maximum extent) of asteroidal mass from the surface of a larger asteroid, to a stable orbit around the Moon for subsequent access by a human crewed mission [8-12]. The Ion Propulsion System (IPS) for ARRM will be used for heliocentric transfer from Earth to the target asteroid, orbit capture at the asteroid, transfer to a low orbit about the asteroid, a planetary defense demonstration after retrieval of the asteroidal mass from the larger asteroid, departure and escape from the asteroid, the heliocentric transfer from the asteroid to lunar orbit, and insertion into a lunar distant retrograde orbit. In addition, the IPS will provide pitch and yaw control of the spacecraft during IPS thrusting. To date, the technology development, performed by the NASA Glenn Research Center (GRC) and the Jet Propulsion Laboratory (JPL), has been focused on an in-house effort to mature the high-power Hall thruster and power processing designs. This work had recently begun the transition to a commercial vendor for the development of an Engineering Development Unit (EDU) Electric Propulsion (EP) string and optional Qualification Model (QM) and Flight Model (FM) hardware delivery in a timeline consistent with the current ARRM implementation. The flight electric propulsion string hardware will be provided as government furnished equipment to the Asteroid Redirect Vehicle (ARV) prime contractor.

As part of a technology maturation plan for the NASA's Hall Effect Rocket with Magnetic Shielding (HERMeS) thruster, two Technology Demonstration Units (TDU-1 and TDU-2) has be subjected to testing in a number of efforts that are planned to increase the Technology Readiness Level (TRL). These efforts include extensive performance, stability, plume characterization, and facility interaction testing of the TDU-1 thruster, which occurred prior to a series of long duration tests to examine the robustness of the thruster. Further details can be found in the partner papers in Refs. [13-19]. The facility interaction testing of TDU-1 will examine the back sputter influence on the performance and wear characteristics, pressure induced effects, and the electrical configuration of the thruster in a ground based conducting vacuum facility (main subject of this paper). The 2,000 hour wear test of the TDU-1 thruster will focus primarily on thruster performance, wear of the thruster and cathode due to interaction with the plasma, plume characterization, thruster stability, and developing an understanding of the back-sputtering effects on Hall thruster wear testing. In a parallel effort, TDU-2 will undergo full environmental and performance testing. The results of the development level environmental testing will be used to improve the final flight system design.

The HERMeS thruster electrical configuration testing main objectives are to determine the most suitable electrical configuration, with respect to the vacuum facility, that simulates how the propulsion system will eventually be operated in space on a NASA mission.

A. Hall Thruster Facility Interaction

As higher-powered Hall thrusters have become more widely planned for future in-space NASA missions, with increased capabilities compared to current state-of-art (SOA) Hall thruster propulsion systems, there are several potential facility interaction considerations that need to be studied and understood in order to realize a low-risk path towards flight. One of the long understood facility interaction concerns with Hall thruster devices is the potential of propellant ingestion from the elevated background pressure of a ground-based vacuum chamber as compared to in-space pressures. This ingested propellant has been previously shown to artificially increase the performance of a Hall thruster over what would be expected in a space environment [20-26]. A relatively new Hall thruster facility interaction concern, identified and discussed in the Hall thruster community, pertains to the electrical interaction of a conducting vacuum facility with the plasma processes of a Hall thruster main plasma discharge, cathode coupling, and the thruster plasma plume [27-35]. Although this electrical interaction has always been present in some form or another, the first experimental examination known to this author was by McDonald in Ref. [36]. McDonald set out to examine how electrons travel from the cathode to the discharge of a Hall thruster and to understand electron transport in the near field region of a Hall thruster. In one of the experiments, McDonald measured a thruster body current to ground when the electrically isolated thruster was connected to facility ground through a calibrated current shunt. By alternating between a floating and a grounded state of the H6 Hall thruster, McDonald was able to determine that the current was composed of collected electrons on the exposed metal components of the thruster. This effect is analogous to a floating Langmuir probe. The full implications of the electrical configuration of a Hall thruster operating in a conducting vacuum facility had not been fully investigated, to the knowledge of this author, until recently by research groups at Georgia Institute of Technology (GIT), Lockheed Martin Space Systems Company,

Aerojet Rocketdyne, and the United States Air Force Research Laboratory (AFRL) [27-35]. The pressure induced and electrical interactions with respect to Hall thrusters will be discussed in further detail in the following sections, with the electrical configuration being the main topic of this paper.

1. Hall Thruster Background Pressure Interaction

During the development of the HERMeS Hall thruster, NASA examined the influence of background pressure on the performance of the TDU-1 thruster and determined that the performance of the thruster remained relatively unchanged, with a slight negative slope, over the range of pressure achievable in Vacuum Facility 5 (VF-5) at NASA GRC [26], shown in Figure 1. The mass flow rate was increased with decreasing pressure to maintain a constant discharge power. Kamhawi in Ref. [26] calculated the influence of ingestion based on the background neutral density flux into the discharge channel of the Hall thruster and determined that the observed change in discharge current with pressure was accountable by loss of ingested neutral xenon atoms that comprised the majority of the background pressure. This suggests that the design of the HERMeS thruster is less sensitive to background pressure changes as compared to prior Hall thruster pressure studies [23, 37, 38].

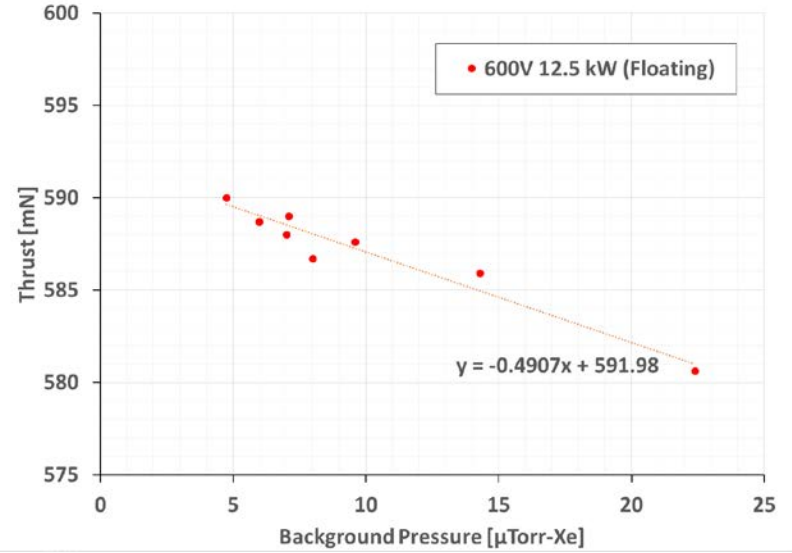

Figure 1. HERMeS TDU-1 performance as a function of background pressure for the 600V 12.5kW throttle condition.

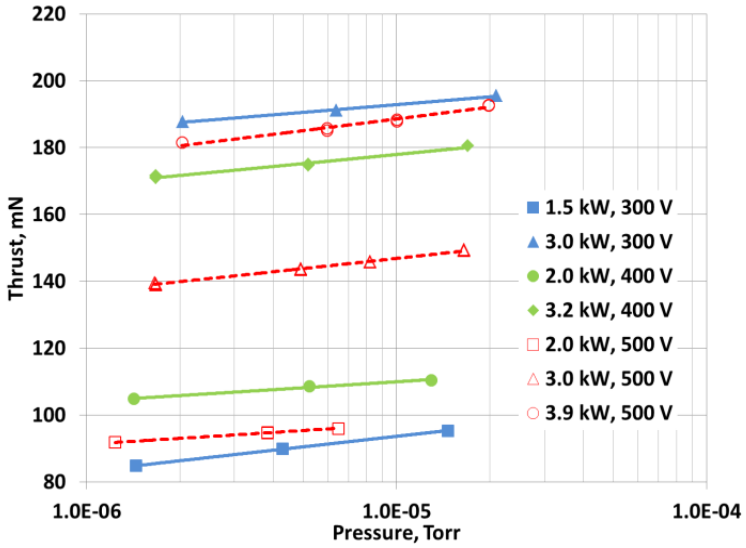

Figure 2. HiVHAC thrust variation as a function of facility background pressure (xenon) during the pressure sensitivity test in NASA GRC's VF-5.

The SPT-100 performance, at a constant power, illustrated a different response to changing background pressures as shown in Ref [23]. The performance of the SPT-100 was approximately constant from 70 to 20 µTorr-Xe then began an exponential decay to approximately 80 mN from 15 to 1.6 µTorr-Xe. Diamant's analysis of the performance and plume data determined the dominant cause of the performance decrease to be a result of the plume divergence increasing with decreasing background pressure. Diamant further theorized that the increased plume divergence was a result of the ionization and acceleration zones moving further downstream towards the exit plane of the thruster at lower facility pressures.

The High Voltage Hall Accelerator (HiVHAC) Hall thruster performance demonstrated a similar shift of the ionization and acceleration zones with background pressure [37, 38] as observed with the SPT-100 in Ref. [23]. As the background pressure was increased, experimental evidence indicated that the ionization and acceleration zones were shifting upstream towards the thruster anode. The HiVHAC Hall thruster also showed similar performance trends as a function of pressure, shown in Figure 2, as was observed with the SPT-100 in Ref. [23]. In addition, calculations indicated that the flow ingestion did not account entirely for the observed change in thruster performance.

The calculated ingestion acceptance area for ionization and acceleration was increased by a factor of two to three times the physical size of the HiVHAC thruster discharge channel area to determine if the data could be matched by an expanded acceptance region outside of the thruster. The results of the artificially expanded region of ionization and acceleration still did not match the observed performance difference with pressure. These calculations indicated that there are other processes besides propellant ingestion that can influence the performance of a Hall thruster as the local background pressure is decreased, which may be related to the change in the plume properties observed by Diamant in Ref [23].

2. Hall Thruster Electrical Configuration

The electrical configuration of a Hall thruster, in relation to a conducting vacuum facility, has been recently identified as a concern that needs to be considered in the development and qualification of new Hall thruster propulsion systems [27-35]. The electrical configuration of a Hall thruster in a conducting ground based vacuum facility can be described in two primary configurations with a newly envisioned third option; 1) the thruster body is electrically tied to the facility ground (Figure 3), 2) the thruster body is isolated from the facility ground and allowed to float with respect to the local plasma potential (Figure 4), and 3) the thruster body isolated from the vacuum facility chamber ground and electrically tied to the floating cathode common (Figure 5) [39]. The first case is the electrical configuration that a vast majority of Hall thruster development and qualification testing has used over the past few decades [40]. In this electrical configuration it has been demonstrated that the propulsion system electrons can travel with the ion beam, as well as finding alternate low-resistance paths through the conducting thruster body and any nearby grounded structure and/or diagnostic equipment in close proximity to the thruster. The electrons traveling through the lower resistance path of the chamber walls meet up with the ions in the beam, and/or Charge-Exchange (CEX) ions, on the walls of the chamber and/or grounded carbon-based beam dump [28, 30, 31, 36].

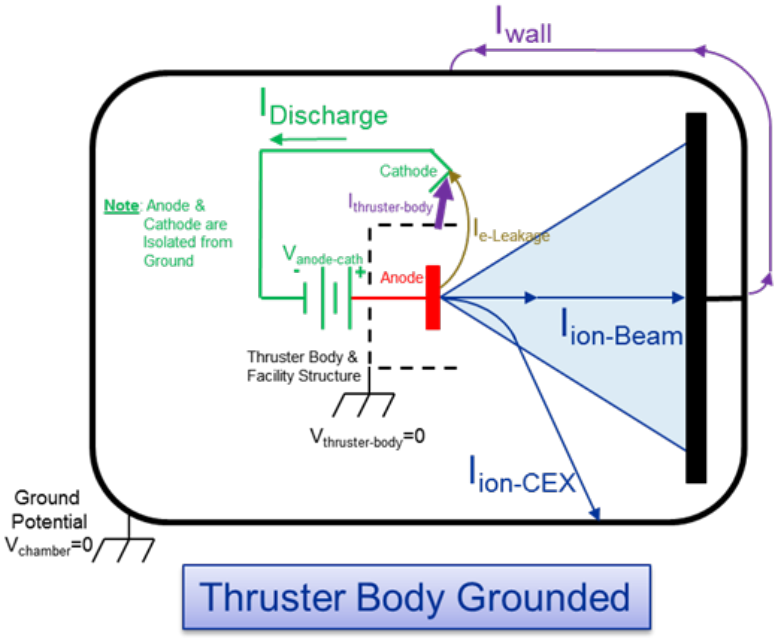

Figure 3. Illustration of a Hall thruster body grounded electrical configurations for ground based Hall thruster testing.

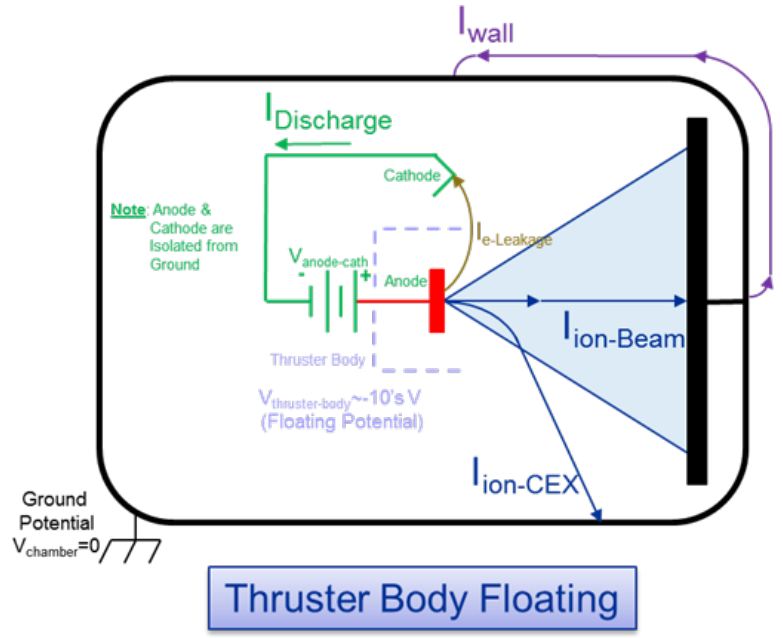

Figure 4. Illustration of a Hall thruster body floating electrical configurations for ground based Hall thruster testing.

The second case is analogous to the electrical configuration employed by current Hall thruster on spacecraft [39, 41], where the thruster body is electrically connected to the spacecraft chassis and spacecraft floats with the local

plasma potential, as shown in Figure 6. In space, a typical Hall thruster is fired away from the spacecraft to minimize the interaction between the plasma plume and the spacecraft. The primary reason for operating a Hall thruster in this manner is to reduce the potential erosion of spacecraft components by the energetic plasma. Since the plasma plume of a Hall thruster in space is fired away from the spacecraft, there is minimum to no chance for the system electrons to recombine with the ions without moving along with the beam and/or CEX ions by ambipolar diffusion. In this case the ion beam and neutralizing electrons are considered well coupled. It is postulated that floating a Hall thruster body in a conducting vacuum chamber can provide a methodology for ground based testing to partially simulate the electrical environment that a Hall thruster will be subjected to in space by forcing the electrons to travel with the beam ions instead of taken a lower resistance path through the conducting vacuum chamber, as illustrated in Figure 3.

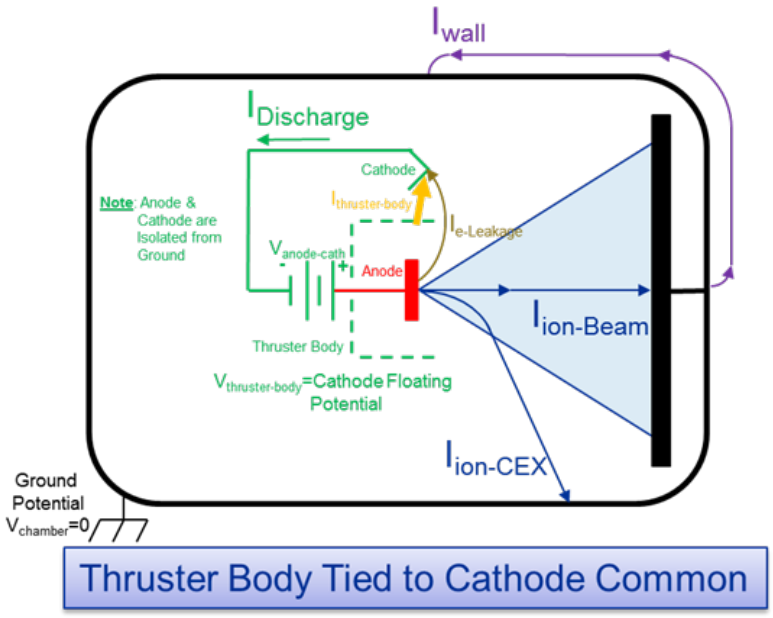

Figure 5. Illustration of a Hall thruster body tied to cathode common electrical configurations for ground based Hall thruster testing.

Several recent electrical configuration studies have determined that allowing a portion of the Hall thruster plume's electrons to travel through the vacuum facility conducting chamber can influence the operation of a Hall thruster [27-35]. The Hall thruster research group at GIT has conducted several experimental campaigns with a T-140 Hall thruster to investigate the coupling of a Hall thruster discharge and plume plasmas with a conducting vacuum chamber [27-31]. Additionally, there has been parallel work conducted by Aerojet Rocketdyne and AFRL on the XR-5 and XR-5A flight Hall thrusters that have resulted in similar findings as those obtained by GIT [32-35]. GIT researchers have determined that a conducting vacuum chamber can influence Hall thruster operation by changing the balance of electron motion in the plume. This configuration can result in a large thruster body negative floating potentials of -20 → -40 V, or higher, with respect to the local plasma potential. The large negative potentials can increase the possible ion erosion of the thruster components, such as the front poles, outside the discharge channel by CEX ions [36, 39]. Additionally, it is likely that a larger negative AC floating potential can be present as a result of the oscillating nature of a Hall thruster. It is theorized that floating a thruster with a large negative potential with respect to the local plasma could result in elevated erosion of thruster components. The negative potential of a floating thruster body will be discussed further in Section III.

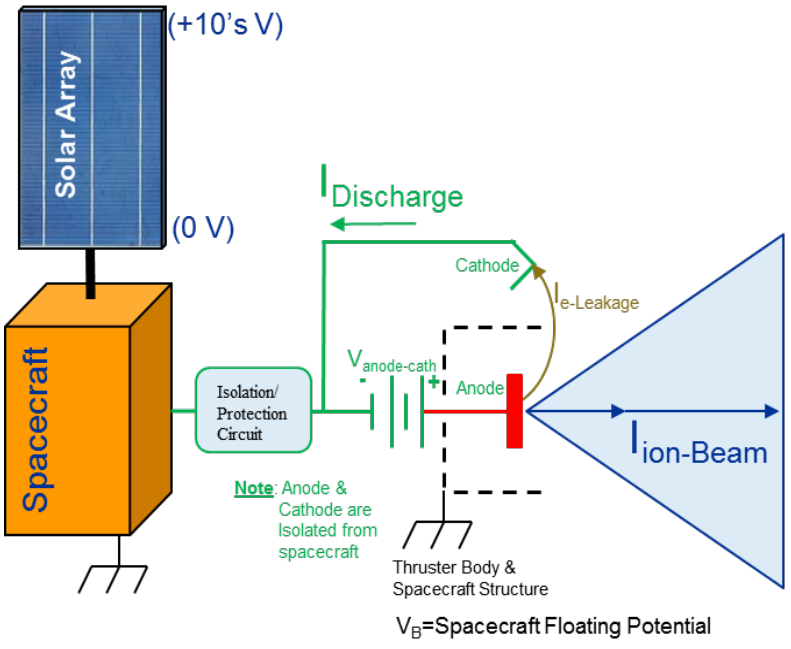

Figure 6. Illustration of a typical Hall thruster propulsion system electrical configuration on a spacecraft.

The third case is a configuration that has been previously employed in anode layer Hall thrusters, which are also known as Thruster with Anode Layer (TAL). This is due to the nature of the thruster configuration in which the guard rings are commonly electrically tied to the cathode common [42-47]. However, it has been recently proposed by Katz in Ref [39], that this electrical configuration could be applied to magnetic layer Hall thrusters, also known as a Stationary Plasma Thrusters (SPT), to limit the floating potential that the Hall thruster body could achieve by repelling the electron thruster body current. It has been suggested that electrically connecting the thruster body to the cathode common will limit the extent of its floating potential to the cathode-to-ground voltage in a grounded vacuum chamber, or to the floating potential of the cathode with respect to spacecraft chassis in space. Even though this proposed electrical configuration would be new for magnetically shielded Hall thrusters, it does represent a previously flown configuration, albeit with much less flight heritage (i.e. TAL).

3. Thruster Exit Plane Boundary Condition

In order to fully examine the influence of a the electrical facility-thruster configuration on the performance, plume, stability, and wear characteristics of the HERMeS Hall thruster, two thruster boundary conditions were included in the test campaign. The thruster boundary conditions for this paper is defined as the exit plane plasma wetted surfaces that can interact with the electrons and ions generated by the plasma discharge. In the first case of a grounded thruster body, discussed in Section I.A.2, one can imagine that a dielectric or conducting interface may play an important role in facility electrical interaction. A dielectric surface may represent a higher resistance path than a conductor in a grounded thruster electrical configuration. A conducting boundary condition in a floating electrical configuration will float to a potential to balance the electron and ion fluxes to a net zero current. This paper will explore the performance and stability of the two boundary conditions with respect to the three thruster-facility electrical configurations discussed in Section I.A.2. A companion paper by Williams will explore the wear characteristics of the two boundary conditions [19].

II. Experimental Apparatus

A. Hall Thruster

The conceptual SEP TDM IPS design utilizes multiple 12.5 kW magnetically-shielded Hall thrusters. To demonstrate high-power, high-specific-impulse performance for the desired mission capability and required lifetime, a joint NASA GRC and JPL team developed the 12.5 kW HERMeS thruster. The HERMeS TDU-1 thruster is shown in Figure 7. The design of HERMeS incorporates technologies developed by NASA over nearly two decades, and is enabled through the use of magnetic shielding to effectively eliminate discharge chamber erosion [3, 48-51]. The result is a significant increase in the operational lifetime of state-of-the-art Hall thrusters, with HERMeS being designed to operate at 3000 s specific impulse with a lifetime exceeding 50 kh.

The HERMeS TDU-1 Hall thruster was fabricated and the first test campaign was completed in 2015. The first test campaign demonstrated thruster performance, verified magnetically shielded operation at high specific impulse, and affirmed that the internally mounted cathode minimizes the effects of facility pressure on performance. Details regarding TDU thruster design, mission-required operating envelope, and test results are detailed in Refs. [3, 48, 49, 52-68].

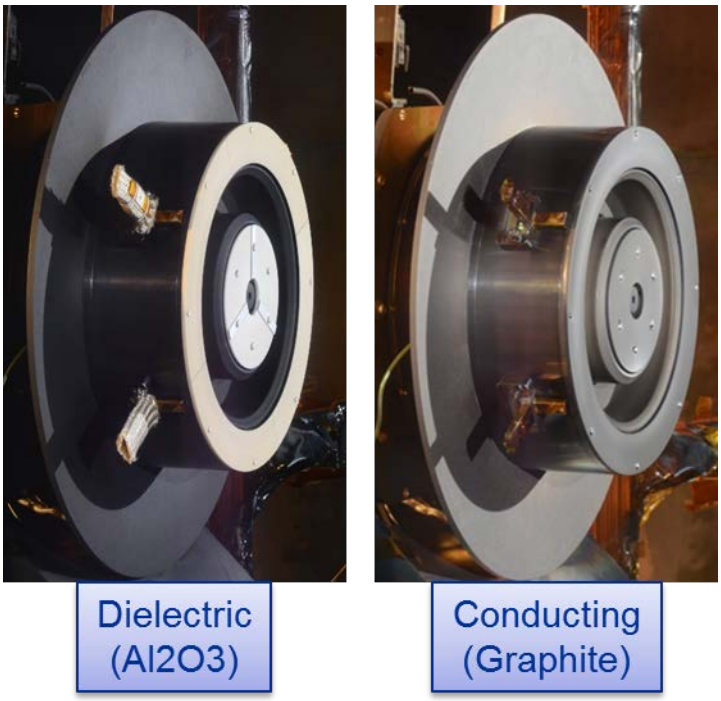

Figure 7. The HERMeS TDU-1 Hall thruster with dielectric (left) and conducting (right) boundary conditions on the exit plane plasma wetted surfaces.

As discussed in Section I.A.2, the TDU-1 thruster could be electrically configured in three different configurations (Grounded, Floating, and Cathode). Changing between each of the electrical configuration was accomplished outside the chamber with the thruster break-out-box. The TDU-1 Hall thruster was configured with two different boundary conditions for the performance and electrical interaction testing described in this paper. The first boundary condition was comprised of a dielectric material (Al2O3) that is commonly employed on flight and development Hall thrusters, shown in Figure 7. The second boundary condition was comprised of a conductor (graphite) which has been used on several development Hall thrusters such as the H6MS, is also shown in Figure 7.

B. Vacuum Facility

Testing of the HERMeS TDU-1 Hall thruster was performed in VF-5 at NASA GRC. Full details on VF-5 can be found in Ref. [69]. The VF-5 main chamber is 4.6 m in diameter, 18.3 m long and can be evacuated with cryopanels and/or oil diffusion pumps. For the test campaign discussed in this paper, the TDU-1 Hall thruster was placed in the main volume of the chamber to ensure that the lowest possible background pressure during thruster operation [70]. Figure 8 shows a picture inside VF-5 from the east end of the chamber. Facility pressure was monitored with three xenon and one air calibrated ion gauges placed in locations to provide accurate background pressure during operation. The location and orientation of the four ion gauges are detail in Figure 9. Ion gauge 3 (IG#3) was employed as the main pressure reading during operation based on the modeling results and experimental experience [26, 70].

Figure 8. NASA GRC VF-5.

C. Power Supplies, Data Acquisition, and Control Systems

For the HERMeS TDU-1 test campaign the thruster was powered with a laboratory power rack that contained the discharge, inner and outer electromagnet, cathode heater, and cathode keeper power supplies. The discharge power supply consists of three 15 kW (1000 V and 15 A) power supplies that were connected in a master-slave configuration. A computer was used to sweep the thruster discharge voltage during the thruster stability characterization test.

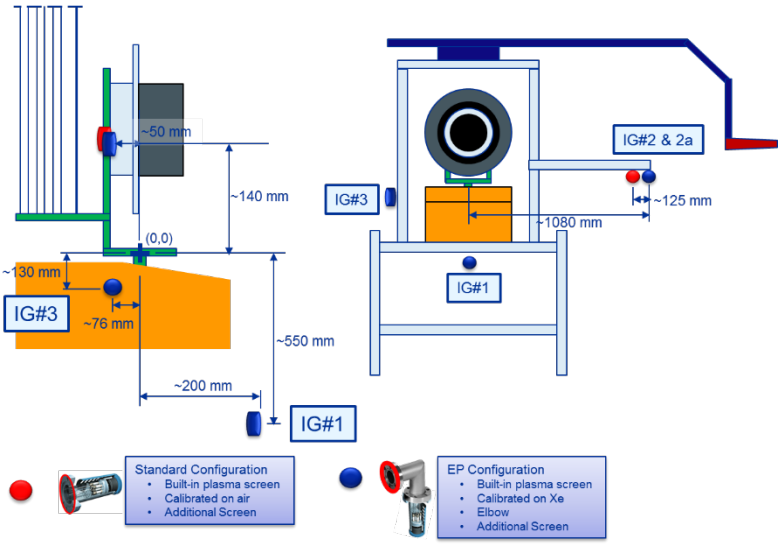

Figure 9. Schematic of the internal ion gauge setup for the TDU-1 test campaign (not to scale).

The data acquisition system used for the TDU-1 electrical configuration characterization was a multiplexed datalogger with computer interface. The datalogger monitored the voltages, currents, temperatures, propellant flow rates, chamber pressure, and thrust at approximately 1 Hz during performance testing. The computer interface had the additional benefit of allowing a number of channels to be monitored with failsafe limits for unattended operation. The uncertainties of the datalogger measurements were ±0.05% for the voltage and current measurements.

D. Flow System

A laboratory propellant feed system was used in the TDU1 test campaign. The feed system supplied xenon to the thruster and was also used to elevate the facility background pressure. The propellant feed system utilized four mass flow controllers (MFC). A 500 and a 100 sccm MFC supplied xenon propellant to the thruster and cathode, respectively. A 200 and 1,000 sccm MFC supplied xenon to elevate the chamber pressure. The MFC calibration curves indicated that the anode and cathode flow rates uncertainty is approximately 1% of the set value.

E. Diagnostics

1. Thrust Stand

The performance characterization of the TDU-1 Hall thruster was measured with an inverted pendulum null-type thrust stand. The NASA GRC high-power thrust stand has an accuracy of ≤1% based on a statistical analysis of the calibration and thrust zero data taken throughout the test campaign. The operation and theory of the inverted pendulum null-type thrust stand are described in detail in Refs. [71-73]. The high-power thrust stand was operated in a null-type configuration, which allows the thruster to remain stationary while testing. The thrust stand is also equipped with a closed loop inclination control circuit, which utilize a piezoelectric element to minimize thermal drift during performance testing. The thrust stand was calibrated in-situ with calibrated masses on a pulley system connected to a stepper motor. The thrust stand was calibrated before and after each performance mapping period.

2. Plasma Plume

A variety of plasma diagnostics were used during the test campaign to map the plasma plume of the TDU-1 Hall thruster. These diagnostics include far-field Faraday Probe (FP), retarding potential analyzer (RPA), accompanying Langmuir Probe (LP), and a Wien filter spectrometer (WFS or **E**x**B** probe). Figure 9 (red box) and Figure 10 shows a diagram and photograph of the plasma plume diagnostics setup in the vacuum facility and are further detailed in Ref. [16].

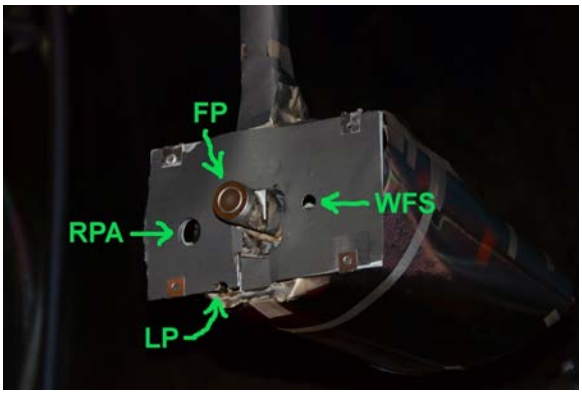

Figure 10. The plasma plume diagnostic system used for the TDU-1 test campaign.

The far-field FP, RPA, accompany LP, and **E**x**B** probe form the probe array. The probe array is mounted on a two-axis polar positioning system. Data collected include current density, ion energy per charge, and species composition as functions of polar angle and distance from the thruster. These data will be used for spacecraft interaction, thruster performance, and facility effect studies. Results of the spacecraft interaction studies will provide guidelines for the design of vehicles that may use HERMeS. The thruster performance studies will be used to characterize and form a baseline for various aspects of the thruster that can influence its performance and lifetime. The results of both studies will also be projected to a space-like environment in order to predict on-orbit thruster and plume characteristics as well as differences from ground-test characteristics.

3. Time Resolved Thruster Telemetry

The temporal behavior of the TDU-1 Hall thruster key parameters were continuously monitored by multiple oscilloscopes. The oscilloscope telemetry included both AC and DC monitoring of the thruster discharge current and voltage, thruster body voltage and current, cathode-to-ground voltage, and other key cathode parameters. The oscilloscopes internal functionally was used to calculate the Root Mean Square (RMS), Peak-2-Peak (Pk2Pk), and mean value where appropriate. The oscilloscope telemetry was fed into the test data acquisition system and recorded on the same time scale as the rest of the telemetry. The logging of the thruster temporal characteristics provided additional information on the high-speed IVB sweep that was demonstrated as useful information when interpreting the thruster stability in Refs. [32, 74]. Additionally a dedicated oscilloscope was used to record five million points of data on the discharge current and voltage for generation of Power Spectrum Density (PSD) plots of the selected operating conditions.

III. Results and Discussion

The TDU-1 thruster was subjected to an extensive set of tests at NASA GRC prior to the start of the long duration wear testing. These tests include standard performance and plume characterization, high-speed maps of thruster discharge current/voltage as a function of applied magnetic field (IVB) maps, magnetic field optimization maps, and

a stability assessment of the TDU-1 thruster. This section provides a summary of the TDU-1 thruster test results in the three thruster electrical configurations and two thruster boundary conditions detailed in Section I.A.2 and an initial interpretation of the presented data. The data presented in the paper are for the 600V 12.5kW HERMeS operating condition. While other throttle conditions were subjected to the same investigation and analysis, the authors believe that the 600V 12.5kW condition provides sufficient information to communicate the findings.

A. Performance Results

As part of the characterization of the TDU-1 Hall thruster, the thruster was subjected to a number of standard Hall thruster performance tests with a goal of understanding the performance and stability of the thruster over a range of operating parameters. The thrust, total efficiency, total mass flow rate, and total specific impulse (Isp) as a function of the magnetic field range of the TDU-1 are presented in Figure 11 through Figure 15, respectively. The key performance parameters, thruster telemetry, and the associated body-to-ground current and voltage are summarized in Table 1. The results shown in Figure 11 through Figure 15 were acquired at a background facility pressure of 4.4 µTorr-Xe, as measured on IG#3. The uncertainty of the thrust measurements for this campaign was statistically calculated from a large sampling of calibration and zero thrust checks and was found to be approximately ±0.6% of indicated thrust value for relative comparison and approximately ±1.8% for absolute measurements. For this discussion, the authors have chosen to use the relative uncertainty, since part of the purpose of this investigation is to examine the influence of the electrical and thruster boundary conditions. The uncertainty for the mass flow rate and electrical telemetry measurements were detailed in Section II.C and II.D. The uncertainty calculations of all of the measurements were propagated through the standard performance equations for total efficiency and specific impulse. The uncertainty bars were applied to two of the boundary cases for illustration purposes in Figure 11 through Figure 15.

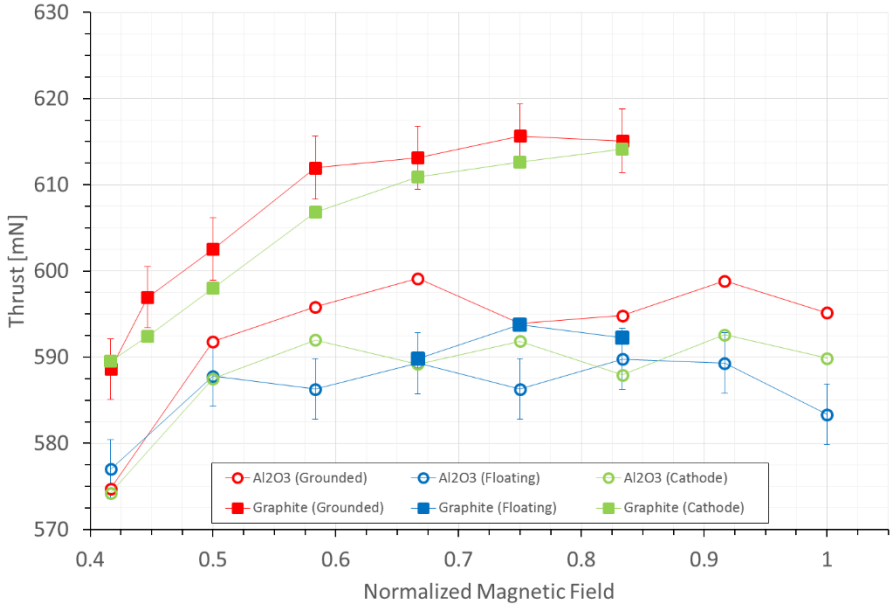

Figure 11. TDU-1 thruster (600V 12.5kW) as a function of normalized magnetic field for the three thruster-facility electrical configurations and the two thruster boundary conditions (statistically based thrust uncertainty is approximately ±0.6%).

The performance results in Figure 11 and Table 1 show several interesting, and important, observations of the TDU-1 in the three electrical configurations and the two different thruster boundary conditions investigated. The most significant finding was the performance decrease of the TDU-1 thruster from the grounded to floating electrical configurations for both thruster boundary conditions. The performance of the TDU-1 decreased by 2% to 4% in thrust, over the magnetic field range of the thruster and for a conducting (graphite) thruster boundary condition between the grounded and floating electrical configurations. The thruster body current was observed to be 2.72 A, 13% of the total discharge current, for the grounded electrical configuration and conducting boundary condition. The thruster body current went to zero, as expected, and the thruster floated to -45 V with respect to the chamber ground with a time-resolved Pk2Pk of -126 V for the conducting boundary condition in the floating electrical configuration. The body of

the thruster floated negative to the local plasma potential to balance out the positive and negative charge collected by the thruster. As for the dielectric (AL2O3) thruster boundary condition, the performance decreased as well but to a lesser extent going from grounded to floating electrical configurations. However, despite the dielectric boundary of the TDU-1 thruster front poles, the thruster still collected 1.36 A, 6.5% of the total discharge current, in the floating configuration. The Al2O3 boundary condition in the floating electrical configuration reached -31 V with respect to the chamber with a time-resolved Pk2Pk of -78 V.

Table 1. TDU-1 600V 12.5kW thruster electrical and boundary condition telemetry.

	Thruster Config.	Electrical Config.	Thrust [mN]	Total Efficiency	Total Mass Flow Rate [mg/s]	Id _RMS [A]	Id_Pk2Pk [A]	Thruster Body Current [A]	Thruster Body Voltage [V]	Thruster Body Voltage RMS [V]	Thruster Body Voltage Pk2Pk [V]
600V 12.5kW	Graphite	G	613	68.2%	22.06	3.98	18.6	2.73	0	-3	-22
		F	590	64.5%	21.56	3.38	13.2	0	-45	-53	-126
		Cath	611	67.8%	22.02	3.98	15.8	1.83	-9	-12	-36
	Al2O3	G	599	66.7%	21.53	3.48	12.2	1.36	0	-2	-14
		F	589	64.8%	21.43	3.19	12	0	-31	-38	-78
		Cath	589	64.6%	21.50	3.42	11.8	0.81	-10	-11	-30

The dielectric boundary condition result, while not expected, is understandable after further consideration is given to TDU-1 magnetic field separatrix topology and that only the downstream face of the thruster was isolated from the plasma and not the sides or the radiator of the thruster (Figure 12). For the TDU-1 Hall thruster with concentric electromagnetic coils, the magnetic field lines from the discharge region of the thruster do not necessarily terminate on the dielectric front pole surface, and may intersect with conducting thruster surfaces. It is expected that if all the thruster surfaces were isolated from the plasma then the collected body current would go to zero for the grounded electrical configuration. Additionally, if the thruster separatrix terminated on a dielectric surface, then the collected body current should be close to zero. The dielectric covered H6MS, with a thruster separatrix that terminates on the outer face of the thruster (Figure 12), recently demonstrated close to zero body current in the grounded electrical configuration in Ref. [39].

The significance of these observations pertain to the classical method that flight Hall thrusters have been qualified and acceptance tested compared to the typical method that Hall thrusters are flown on spacecraft (Figure 6). As discussed in Section I.A.2, the thruster body is electrically connected to the spacecraft chassis and the chassis is allowed to float relatively to the local plasma potential. The results presented in Figure 11 suggest that a Hall thruster may have a slight to moderate performance decrease in space compared to the ground based testing that is not related to propellant ingestion effects on performance, as discussed in Section I.A.1. Another interesting interpretation of the data presented in Figure 11 is that the configuration of the Hall thruster external surfaces, dielectric or conductor, may account for the lack of performance change in the SPT-100 pressure study in Ref. [23] when switched between

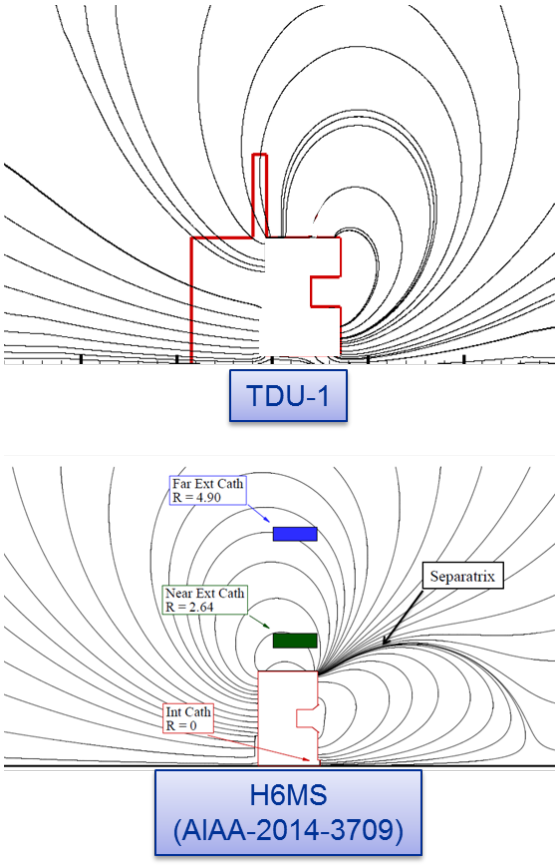

Figure 12. Illustration of the two types of magnetic field topologies and their associated separatrices.

grounded and floating configurations. The SPT-100 is configured in a typical Hall thruster flight configuration with a dielectric coating on the plasma wetted downstream surfaces. The results presented in Figure 11 for the TDU-1 Hall thruster indicate that the performance differences between the grounded and floating electrical configurations, while greater than the measurement uncertainty, were still small. This issue may be further masked by the difference of the magnetic field separatrix of the SPT-100, which is comprised of five electromagnetic coils, compared to the TDU-1 concentric electromagnetic coils. Additionally, the locations of the cathode and thruster separatrix have been shown to play a role in performance with decreasing background pressure [28, 30, 31, 75]. Given the differences listed here, it is probable that the configuration difference between the two thrusters might mask and/or result in decreased sensitivity to the electrical configurations for the SPT-100. However, without knowledge of the potential thruster body current in the SPT-100 when connected to facility ground, it is difficult to fully correlate the two sets of data. The SPT-100 dielectric plasma wetted surfaces and the topology of the separatrix may have resulted in shielding the thruster from the system's electrons finding a low resistance path through the thruster body to the conducting vacuum chamber.

Another set of interesting observations from Figure 11 and Figure 14, is the initial conclusion that can be drawn from the total mass flow rate required and the measured performance of the TDU-1 at the three thruster-facility electrical configurations and the two thruster boundary conditions. Since the grounded electrical configuration provided the highest measured thrust at 600V 12.5kW (fixed discharge current) and had the highest mass flow rate, implies that the thruster in the grounded configuration had the highest current utilization efficiency of the three different configurations tested (the thruster body tied to cathode common will be discuss later). While, for the floating configuration with conducting boundary condition, and the dielectric boundary at the three thruster-facility electrical configurations, had a lower measured thrust and lower total mass flow rate to hit the 20.83A discharge current. This implies that in these configurations a larger portion of the thruster discharge current was in the form of electrical leakage current, or non-propulsive ion current. These results will be further discussed and correlated with the plasma plume results presented in Section III.B.

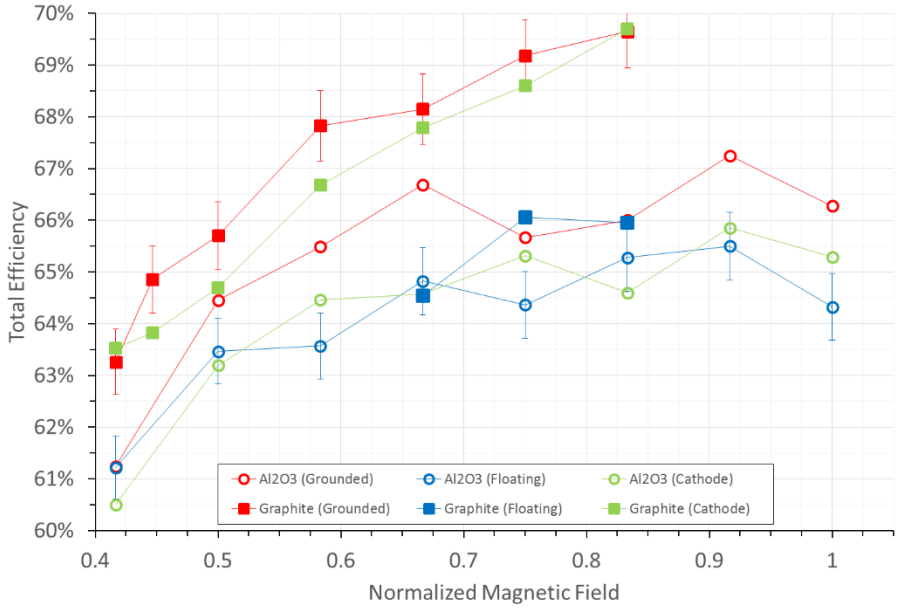

Figure 13. TDU-1 total efficiency (600V 12.5kW) as a function of normalized magnetic field for the three thruster-facility electrical configurations and the two thruster boundary conditions (uncertainty of approximately ±1.17%)

The total Isp results for the thruster in all of the thruster-facility electrical configurations and thruster boundary conditions are comparable for the range of thruster magnetic fields considered (Figure 15). However, Figure 15 does provide insight on the magnetic field range that the TDU-1 thruster should be operated in order to maximize the performance of the thruster. The results indicate that operating the TDU-1 thruster at the upper range of the magnetic field provides better performance and reduced propellant requirements, although only a slight improvement is gained.

As for the newly proposed thruster electrical configuration, cathode electrically connected to the cathode common of the Hall thruster system (Figure 5), the performance results in Figure 11 through Figure 15, and Table 1, indicate very promising performance results for the conductive boundary condition. The thrust, total efficiency, and total mass flow rate approached the grounded electrical configuration results for the conducting thruster boundary condition.

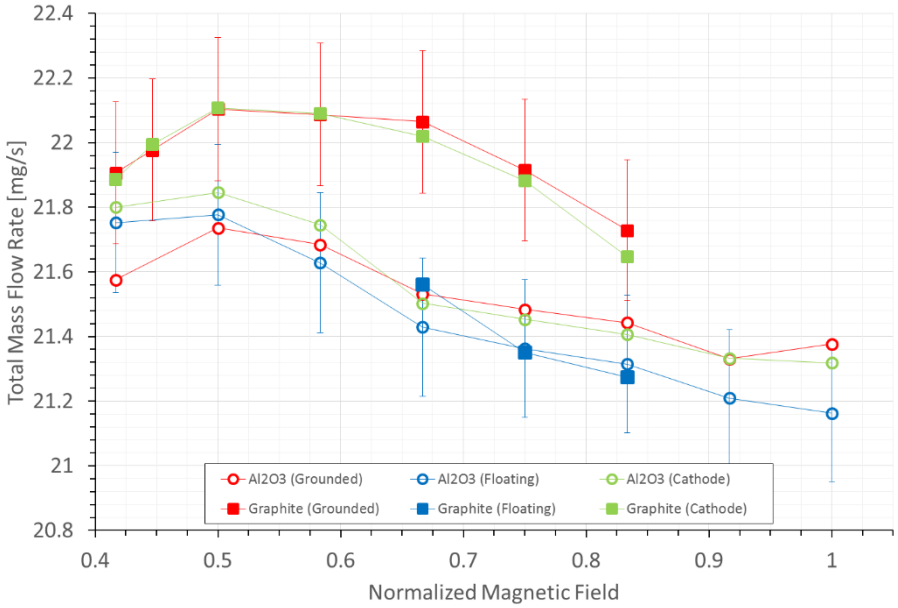

Figure 14. TDU-1 total mass flow rate (600V 12.5kW) as a function of normalized magnetic field for the three thruster-facility electrical configurations and the two thruster boundary conditions (uncertainty of approximately ±1%)

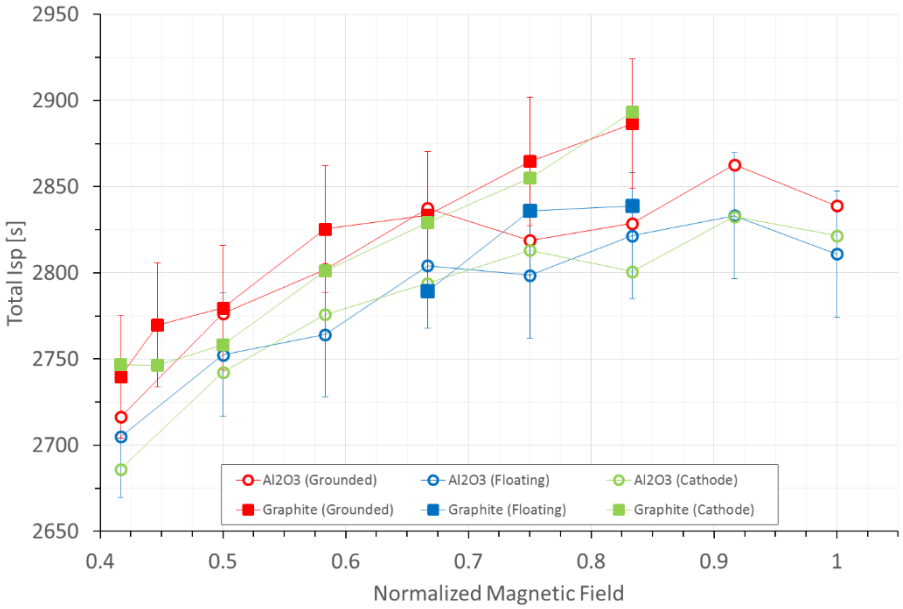

Figure 15. TDU-1 total Isp (600V 12.5kW) as a function of normalized magnetic field for the three thruster-facility electrical configurations and the two thruster boundary conditions (uncertainty of approximately ±1.3%)

However, unlike the grounded electrical configuration, the system electrons cannot take a low resistance path through the conducting vacuum chamber and recombine with the primary and/or CEX ions at the beam dump and/or chamber walls as shown in Figure 3. The cathode tied electrical configuration does result in electrons still being

collected by the thruster body; however, since the thruster body is electrically connected to the cathode, the collected electrons are forced back through the hollow cathode [39], as shown in the simple circuit diagram in Figure 16. Any potential power loss from this configuration has already been accounted for in the ratio of propulsive power to the system's total power. As indicated in the results presented in Figure 11 through Figure 15, the thruster body electrically connected to the cathode common provides a similar physical process, and performance gains, as the grounded electrical configuration without the need for a large conductive shell to be surrounding the propulsion system. The thruster floating potential, in the cathode tied electrical configuration, is limited to the cathode floating potential, approximately -10 V to the ground for the data presented in this paper in a ground vacuum facility (cathode-to-ground voltage). As shown in Table 1, the steady state mean thruster potential was -9 V with a Pk2Pk of -36 V for the conducting graphite boundary condition and -10 V mean and -30 V Pk2Pk for the dielectric Al2O3 boundary condition in the cathode tied electrical configuration. While both the mean and Pk2Pk negative thruster body potential will increase any likely front pole erosion, it is still an approximately 80% decrease in mean and Pk2Pk negative potentials for the conducting graphite boundary condition as compared to the floating electrical configuration. The dielectric Al2O3 thruster boundary condition demonstrated a slightly smaller thruster potential decrease of ~66% for the mean and Pk2Pk from the floating electrical configuration to the cathode tied electrical configuration. The cathode tied to the isolated thruster body suggests that a Hall thruster propulsion system will most likely have a greater resistance to pole erosion than in a typical flight configuration (Figure 6). It is important to note that pole erosion is not a typical concern for current flight Hall thruster because of the required lifetimes.

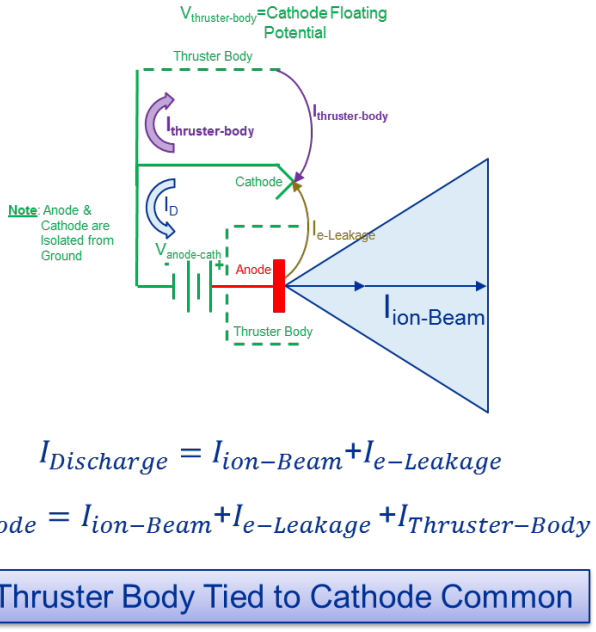

Figure 16. A partial circuit diagram of the thruster body electrically tied to the cathode common.

At this stage of development of the HERMeS propulsion system, the thruster body electrically connected to the cathode common and isolated from the spacecraft chassis is a feasible option for future spacecraft architecture. The results for the dielectric thruster boundary condition, while not as definitive with the conducting configuration, still has noticeable benefits. The primary benefit is the knowledge of the electrons collected by the thruster body will be directed through the cathode and not allowed to find a low resistance path through the chamber, which will be absent during in-space operation.

B. Plasma Plume Characterization Results

The second portion of the TDU-1 characterization was to map the plume of the thruster at the three thruster-facility electrical configurations and the two boundary conditions. Correlating the plume and performance results can provide further insight into the processes of the TDU-1 Hall thruster. As described in Section II.E.2 earlier, the TDU-1 thruster was mapped with a FP, RPA, LP, and an **E**x**B** probe.

A comparison of the ion beam profile from the Faraday probe is shown in Figure 17. The conducting boundary (graphite) for the grounded and cathode tied electrical configurations have very similar profiles. The floating electrical configuration with the conductor boundary condition behaves similar to all three electrical configurations for the dielectric boundary condition. The momentum-weighted plume divergence angle for the six configuration were found using the methodology discussed in Ref. [16] and is tabulated in Table 2. The momentum-weighted plume divergence angle did not change much between the thruster configurations for the conducting graphite boundary condition. There is slightly more of a change in the momentum-weighted plume divergence angle for the dielectric boundary conditions. The floating electrical configuration had a slightly higher divergence than the grounded and cathode tied configuration with the lowest divergence observed in the grounded configuration (relative comparison). Although the performance of the TDU-1 with the conducting boundary condition and floating electrical configuration was within the family of the dielectric results, the plume divergence was still less for the conducting boundary condition.

The RPA provided more interesting and informative results for the plume high-energy ion cone, which is defined as the polar angle in which primary ion energies (~600 eV) are measured. The ion energy per charge versus polar angle is plotted for each of the six electrical and boundary conditions in Figure 18, while the final results are tabulated in Table 2. The first observation from the high-energy ion cone results is the dielectric boundary condition has a smaller cone of primary ions than the conducting boundary by 5° to 20° for each electrical configuration. The results imply that there is a smaller primary ion divergence for the floating electrical with a conducting boundary and the three electrical configurations with a dielectric boundary condition. If thruster-spacecraft interaction is a primary concern for spacecraft architects and mission planners, then it might be advantageous to use the dielectric and/or floating electrical configuration for the continued thruster development towards flight hardware. However, there are other concerns that need to be weighed and assessed alongside the plume results, such as thruster component erosion and thruster performance. There is a HERMeS TDU-1 companion paper that details the erosion results of the conducting and dielectric front pole boundary conditions of the thruster and can be found in Ref. [19].

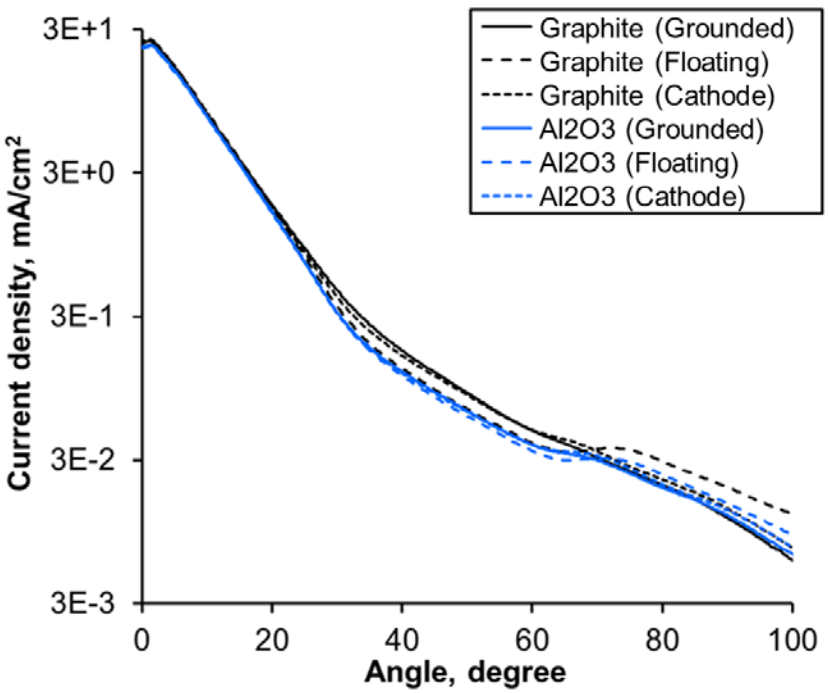

Figure 17. Ion current density profiles for the six configuration tested (only the one side is presented for comparison).

Table 2. Summary of the plume results for the TDU-1 operating at 600V 12.5kW

	Thruster Config.	Electrical Config.	Plume Momentum-Weighted Divergence Angle	Plume High Energy Ion Cone	Charged Species Fractions		
					Xe^{+}	Xe^{++}	Xe^{+++}
600V 12.5kW	Graphite	G	19.3°	75-90°	84.0%	12.1%	3.9%
		F	19.2°	60-65°	86.9%	9.7%	3.4%
		Cath	19.3°	70-75°	86.1%	10.1%	3.8%
	Al2O3	G	19.5°	60-65°	87.9%	8.6%	3.6%
		F	19.8°	55-60°	87.0%	9.3%	3.7%
		Cath	19.6°	60-65°	87.1%	9.1%	3.8%

One final plasma plume characterization results are the measured species fraction measured by the **E**x**B** probe along the centerline of the TDU-1 thruster at 600V 12.5kW. The **E**x**B** probe results are tabulated in Table 2 and indicates that in general the conducting boundary condition in the three electrical configurations has a lower fraction of singly-charge ions and greater double-charge ions than the dielectric boundary condition. It should also be noted that the for the triply-charge ions, the species fraction indicated no significant changes between the six configurations examined during this testing campaign. In the conducting (graphite) boundary condition the singly-charged species

fraction increased by approximately 3% when changed from grounded to floating electrical configurations. As discussed earlier, in Section I.A.2 and Figure 6, the floating electrical configuration may represent the most space like configuration and the results in Table 2 indicate that the floating and cathode tied electrical configurations for both boundary conditions provide the most singly charge species fraction. Decreasing the doubly- and triply-charged ion species fractions provides easier integration into the spacecraft since multiply-charged propellant ions can cause more sputter/erosion damage than singly-charged ions. Another important observation from Table 2 is that the dielectric boundary conditions provides the least amount of multiply-charged ions by as much as a 1%. While a relatively small difference between the two boundary conditions, concerns for a spacecraft integration could benefit from a marginal decrease in the high-eroding doubly-charge ions population that a floating and/or dielectrically covered Hall thruster provides.

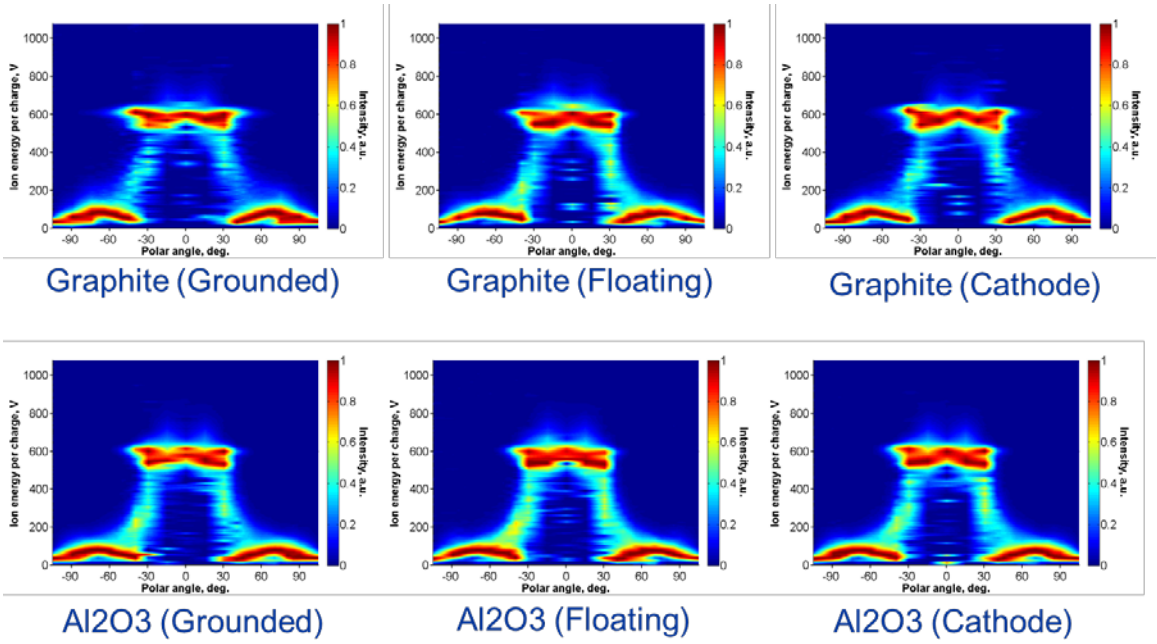

Figure 18. Ion energy per charge vs polar angle plots for each of the six electrical and boundary conditions for the TDU-1 Hall thruster.

C. Thruster Stability Characterization Results

The third portion of the TDU-1 characterization was to map the thruster stability, discharge current and voltage, by examining the time resolved thruster telemetry as a function of the applied magnetic field and at the three thruster-facility electrical configuration and the two boundary conditions. Correlating the stability results with the performance and plume results can provide further insight into the operation of the TDU-1 Hall thruster. The RMS and Pk2Pk of the discharge current and voltage as a function of applied magnetic field are presented in Figure 19 and Figure 20, respectively. The stability results provide some informative trends for the six configuration examined during this testing campaign. The discharge current RMS as a function of applied magnetic field was higher for the conducting boundary, for both the grounded and cathode tied electrical configurations, compared to the floating electrical configuration with conducting boundary condition and all three electrical configurations for the dielectric boundary conditions. This is further evidence that the floating electrical configuration with conducting boundary was operating in a similar manner as the dielectric boundary condition in the three electrical configurations. However, the RMS of the discharge voltage indicates a different interpretation of the two boundary conditions in that the voltage RMS increased for the dielectric results, as compared the conducting boundary condition, from 65% to 85% of the applied magnetic field capabilities of the TDU-1.

The second set of stability plots examine the Pk2Pk of the discharge current and voltage, shown in Figure 20. The discharge current Pk2Pk indicates that the conducting boundary condition, at the grounded and floating electrical configurations, is higher than all three electrical configurations for the dielectric boundary condition. The floating electrical configuration with the conducting boundary condition falls within all three electrical configurations for the dielectric boundary conditions. The discharge voltage Pk2Pk indicates a different response to the applied magnetic field than has been observed with the rest of the data presented in this paper. There appears to be higher Pk2Pk

discharge current and voltage oscillation for the conducting boundary condition at low magnetic fields and then only the grounded electrical configuration with the dielectric boundary condition increases at the highest applied magnetic fields. The significance of these observations is still being assessed, however, one can draw a preliminary conclusion on the configuration and operating regime that the TDU-1 Hall thruster should be operated from a stability point of view. While the results are different over the range of applied magnetic fields, both sets of data indicate that the thruster is stable in all six configurations and that other consideration can be weighed higher in the assessment process.

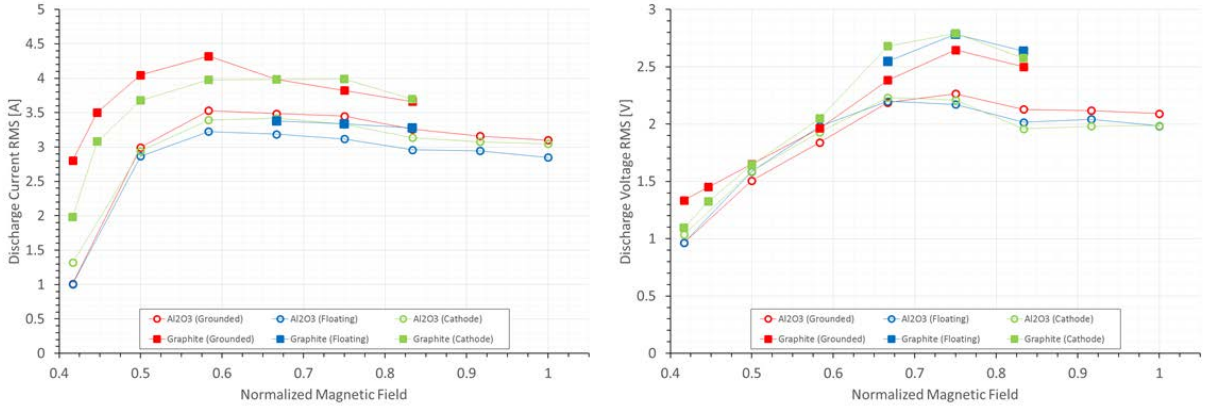

Figure 19. The discharge current and voltage RMS as a function of applied magnetic field.

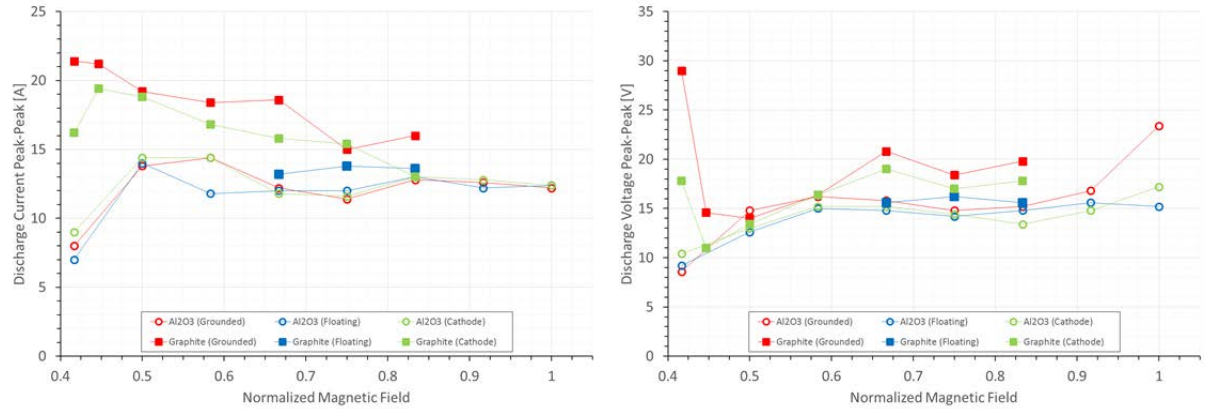

Figure 20. The discharge current and voltage Pk2Pk as a function of applied magnetic field.

To further understand the stability of the TDU-1 Hall thruster the team employed a high-speed discharge voltage sweeps at various applied magnetic fields and at a fixed mass flow rate and recorded the discharge current response. This Hall thruster diagnostic technique is referred to as a high-speed IVB map and has successfully been used by other Hall thruster investigations [32, 37, 38]. The IVB maps for the three electrical configurations and two boundary conditions are shown in Figure 21 to Figure 23. These IVB maps can contain a vast amount of information on the operating characteristics of a Hall thruster and can provide a good sense of stability range as well as help assess the operational margins available. The first IVB comparison for the grounded electrical configuration is shown in Figure 21 and indicates that both boundary conditions have a mode switch around a discharge voltage between 400 V and 450V where the discharge current RMS values jump from ~1 A to ~4.5 A. Additionally, the conducting boundary condition has one step increase (~ 4.9 A) in the RMS contour plot compared to the dielectric contour plot. However, in the cathode tied electrical configuration IVB map (Figure 23) the RMS values of the discharge current remain approximately the same between the two boundary conditions.

A mode switch could represent a change in the plasma plume profile, a change in the location of the ionization and acceleration region, and/or the ionization processes for the Hall thruster. However, since the mode switch occurs for all six configuration investigated in the test campaign at approximately the same discharge voltage, it is more likely a result of Hall discharge process change at evaluated voltages. A comprehensive study over a variety of Hall

thruster design practices and scaling could determine if this is a fundamental feature of a Hall thruster or a particular feature of the HERMeS design.

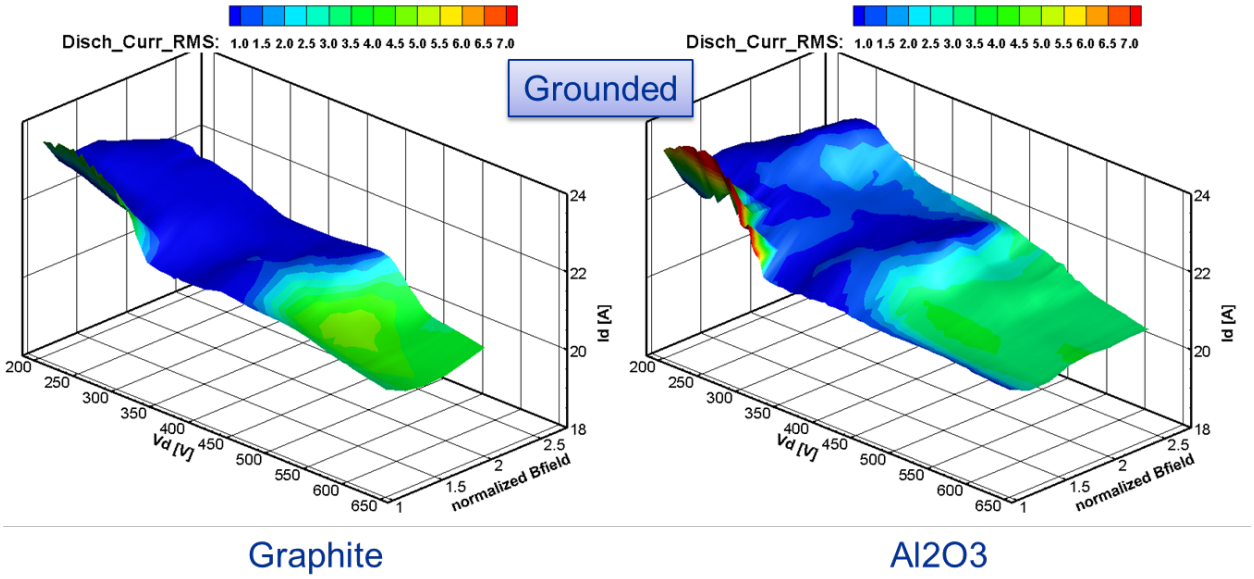

Figure 21. IVB maps for the TDU-1 at 600V 12.5kW in the grounded electrical configuration for the two boundary conditions.

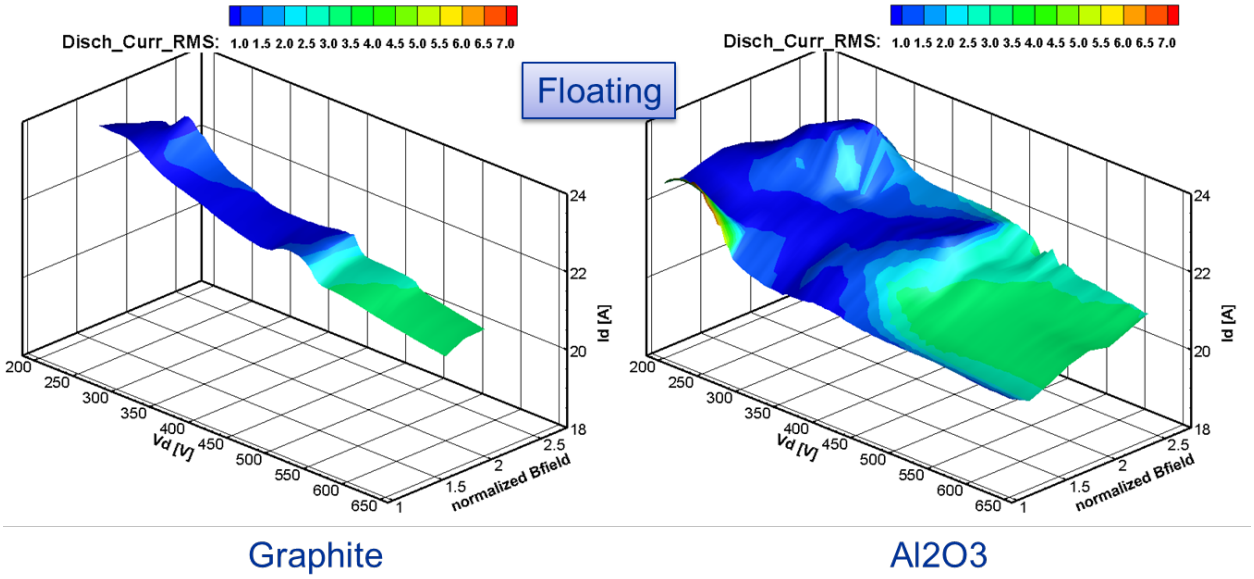

Figure 22. IVB maps for the TDU-1 at 600V 12.5kW in the floating electrical configuration for the two boundary conditions (limited data available for the graphite boundary condition in the floating electrical configuration).

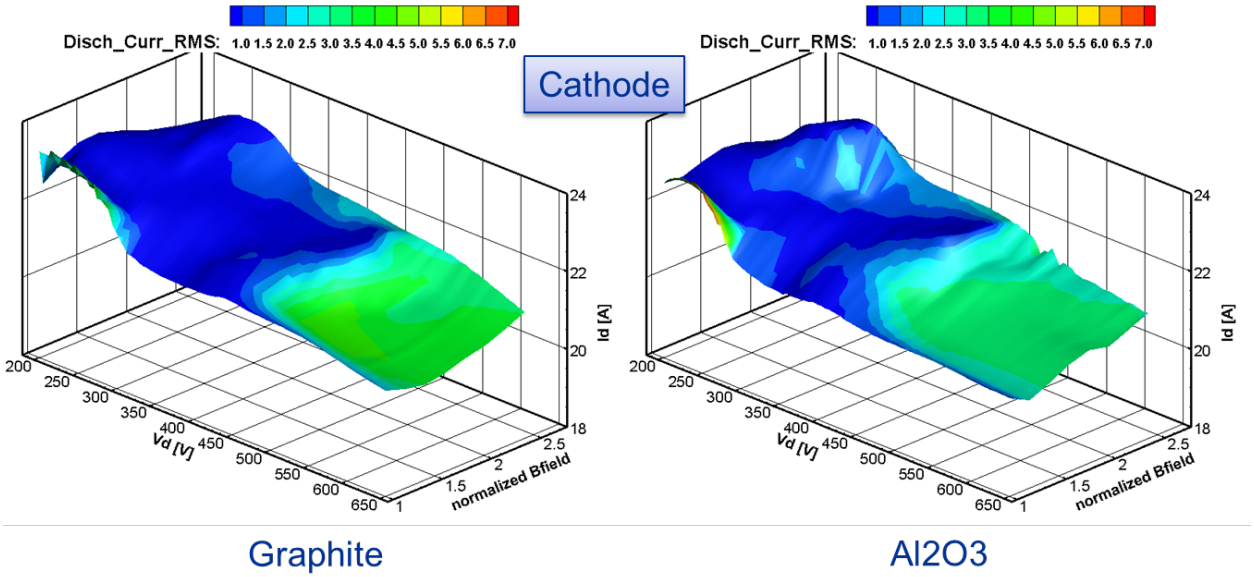

Figure 23. IVB maps for the TDU-1 at 600V 12.5kW in the cathode tied electrical configuration for the two boundary conditions.

The final set of telemetry that was acquired during the test campaign was PSD of the TDU-1 discharge current at each of the six different configurations investigated. The PSD of a Hall thruster discharge current is a method for characterizing the oscillating nature of a thruster and has been used in the past to observe its primary oscillation frequency, referred to as the "breathing mode". The breathing mode oscillation of a typical Hall thruster has been described as an axial ionization wave in the discharge channel and was first described by Fife in Ref. [76] by the following relationship:

$$2\pi f_i = \frac{\sqrt{V_{ion}V_n}}{L_{Discharge}}, \qquad \textbf{Equation (1)}$$

$$L_{Discharge} = \frac{\sqrt{V_{ion}V_n}}{2\pi f_i} \sim \frac{Constant}{f_i}, \qquad \textbf{Equation (2)}$$

where f_i is the primary oscillation frequency of the Hall thruster, V_{ion} is the accelerated ion exit velocity, V_n is the thermal speed of the neutral propellant entering the discharge channel, and $L_{Discharge}$ is the length of the ionization and acceleration regions of the discharge channel. The relationship in Equation (1) can provide a means to quantify weather the electrical configurations and/or the boundary conditions explored in the test campaign caused the discharge to move in the discharge channel. Rearranging Equation (1) for $L_{Discharge}$ and assuming that the ion exit velocity (confirmed by RPA most probable voltage data for the six configurations) and the neutral propellant (assume the TDU-1 thermal loading unchanged for the anode) remain constant between the six configurations, therefore any changes in the primary oscillation frequency may indicate a shift in the discharge location and/or length, shown in Equation (2).

The PSD for the dielectric boundary condition and the three thruster-facility electrical configurations is shown in Figure 24. The grounded configuration had the lowest primary oscillating frequency followed by the cathode tied and then the floating configurations. The largest change was from the grounded to floating configuration and implies, from Equation (2), that the ionization and acceleration zones length in the discharge channel decreased in the floating configuration as compared to the grounded configuration. This could imply that the plasma potential distribution changed between the grounded and floating configurations and could be confirmed by near field plasma potential measurements, not conducted in this testing campaign. An interesting result is the change in the primary oscillation frequency between the cathode-tied and the grounded configurations. The small decrease in the performance results, shown in Figure 11, between the grounded and cathode tied configurations implied a similar operation characteristics between the two configurations. However, there is a clear shift in the PSD between the two cases. The results in Figure 24 suggest that additional diagnostic measurements will need to be employed to examine the physical processes occurring between the electrical configurations.

The PSD for the conducting boundary condition and the three thruster-facility electrical configurations is shown in Figure 25. The observed trends in the conducting case are similar to the dielectric configuration. One difference in the conducting versus dielectric boundary conditions is that aside from the shift in frequency, the amplitude of the frequency peaks grew from grounded to cathode to floating electrical configurations. A similar trend was observed in the discharge voltage RMS and Pk2Pk in Figure 19 and Figure 20, respectively.

Finally a comparison of the PSD from both dielectric and conducting boundary conditions in the thruster-facility floating configuration is shown in Figure 26. There is an increase in primary oscillating frequency from the dielectric to conducting boundary conditions; however, the amplitude remained approximately the same. The increase in a frequency for the conducting boundary condition implies a decrease in the ionization and acceleration region length in the discharge channel. Combining the observation from Figure 26 and Table 2, one can tentatively conclude that because the high-energy primary ion cone was smaller for the dielectric boundary condition, that more of the ionization and acceleration occurred deeper in the discharge channel. This would effectivity prevent higher angle divergent ions from escaping into the plume.

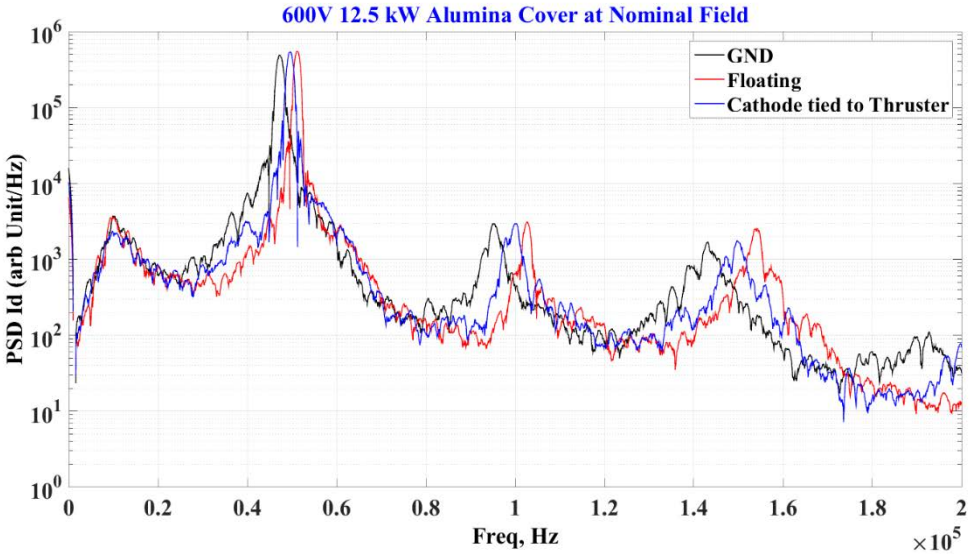

Figure 24. The TDU-1 discharge current PSD for the dielectric boundary condition and the three electrical configurations.

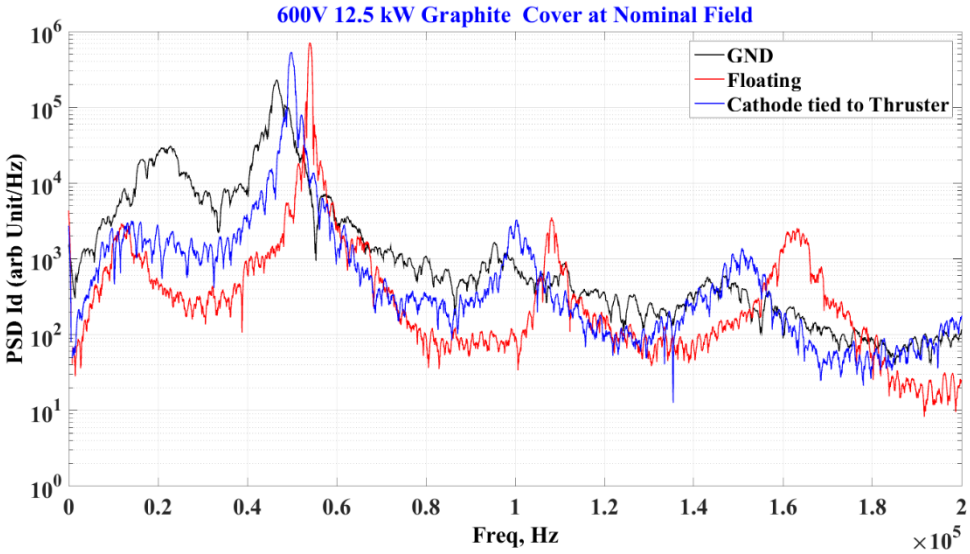

Figure 25. The TDU-1 discharge current PSD for the conducting boundary condition and the three electrical configurations.

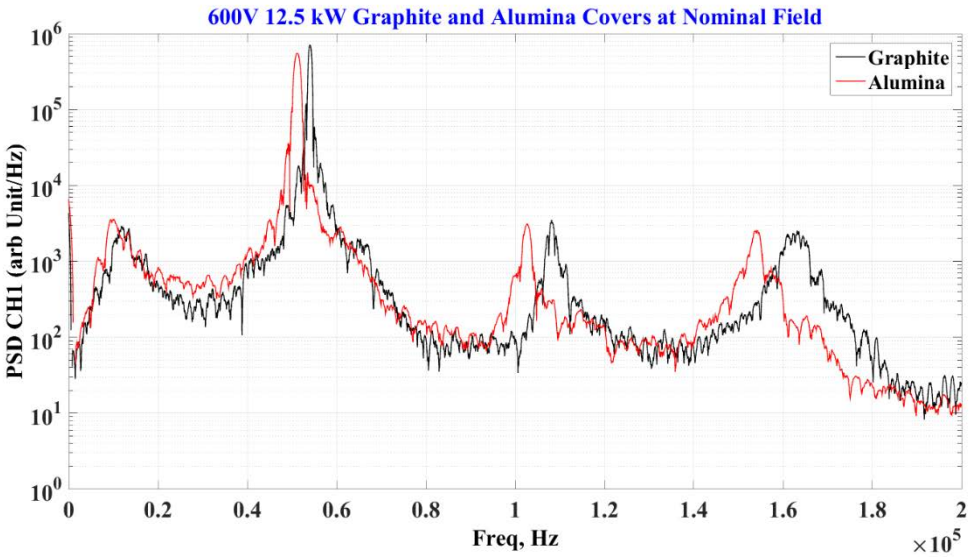

Figure 26. A comparison of the TDU-1 PSD in the floating electrical configuration for the dielectric (Al2O3) and conducting (graphite) boundary conditions.

IV. Conclusion

The NASA 12.5 kW HERMeS TDU-1 Hall thruster was successfully characterized in three different thruster-facility electrical configurations with dielectric and conducting boundary conditions. The characterization included performance, plume, and stability assessments. The performance results indicated the highest performance was achieved in the grounded and conducting configuration. However, telemetry indicated a large electron current, approximately 10% of the discharge current, from the thruster body to the facility ground in this configuration. Recent Hall thruster investigations have found that a grounded Hall thruster chassis in a conducting vacuum facility can syphon a portion of the electrons from the system and allow them to travel through a lower resistance path of the chamber and recombine with the ion beam at the beam dump and/or chamber walls. This configuration cannot be replicated in space and might result in the Hall thruster operating differently in flight. The plume results provide key information in assessing the performance characterization in the six configurations examined. The high-energy primary ion cone was 5° - 20° narrower for the dielectric boundary condition compared to the conducting boundary condition. The charge species fraction for the dielectric boundary condition showed a slight improvement of singles-to-doubles ratio compared to the conducting boundary condition for all three electrical configurations. The stability assessment of the three different thruster-facility electrical configurations with dielectric and conducting boundary conditions provided additional information on the operation of the thruster. The TDU-1 was slightly less oscillatory in the dielectric boundary conditions for all thruster-facility electrical configurations. The PSD of the six configurations examined in the paper indicate that changing the thruster boundary condition and/or the thruster-facility electrical configuration can influence the ionization and acceleration regions of the TDU-1 Hall thruster. The work covered in this paper also examined a potential new thruster electrical configuration, thruster chassis electrically connected to the cathode common, that may provide solutions to ground based development and testing and how they relate to in-space operation. The results presented in this paper are only part of the information gained on the TDU-1 thruster and will be used with other information to help direct the final thruster configuration for future NASA missions.

Acknowledgments

The authors would like to thank the Space Technology Mission Directorate through the Solar Electric Propulsion Technology Demonstration Mission Project for funding the joint NASA GRC and JPL development of the HERMeS tTDU-1 thruster and this work. We thank Christopher M. Griffiths, Lauren K. Clayman, James L. Myers, Li C. Chang, Dale A. Robinson of the NASA GRC and Benjamin Jorns, James E. Polk, Michael J. Sekerak, Ryan Conversano of the JPL for work on the SEP TDM HERMeS Hall thruster. And we like to thank Michael Swiatek, Chad Joppeck, Kevin L. Blake, George P. Jacynycz, Thomas A. Ralys, and Terrell J. Jensen for the fabrication, assembly of the test setup, and operation of the vacuum facility.

References

[1] B. K. Smith, M. L. Nazario, and C. C. Cunningham, "Solar Electric Propulsion Vehicle Demonstration to Support Future Space Exploration Missions," presented at the Space Propulsion 2012, Bordeaux, France, 2012.

[2] D. H. Manzella and K. Hack, "High-Power Solar Electric Propulsion for Future NASA Missions," presented at the 50th AIAA/ASME/SAE/ASEE Joint Propulsion Conference, Cleveland, OH, 2014.

[3] H. Kamhawi, W. Huang, T. W. Haag, J. Yim, L. Chang, L. Clayman, *et al.*, "Overview of the Development of the Solar Electric Propulsion Technology Demonstration Mission 12.5-kW Hall Thruster," presented at the 50th AIAA/ASME/SAE/ASEE Joint Propulsion Conference, Cleveland, OH, 2014.

[4] B. Spence, S. White, M. LaPointe, R. Takeda, G. Carter, K. Schmid, *et al.*, "Technology Maturation and Advancement Update of the ROSA/MegaROSA Solar Array " presented at the Space Power Workshop, Huntington Beach, CA, 2014.

[5] C. R. Mercer and et. al., "Solar Array Technology Development for Electric Propulsion," presented at the Space Power Workshop, Huntington Beach, CA, 2015.

[6] D. Murphy, M. Eskenazi, J. Spink, M. McEachen, T. Trautt, and M. McClenathen, "MegaFlex Solar Array Development and Test – Results from Phase 1 of the NASA Game Changing Development (GCD) Program for Solar Electric Propulsion (SEP) Solar Array Systems (SAS) Program," presented at the Space Power Workshop, Huntington Beach, CA, 2014.

[7] T. W. Kerslake, "Advanced Solar Arrays for NASA Electric Propulsion Missions," presented at the SciTech 2015, Kissimmee, FL, 2015.

[8] J. R. Brophy and B. Muirhead, "Near-Earth Asteroid Retrieval Mission (ARM) Study," presented at the 33rd International Electric Propulsion Conference, Washington, DC, 2013.

[9] M. Gates, "NASA's Asteroid Redirect Mission Concept Development Summary," presented at the IEEE Aerospace Conference, Big Sky, MT, 2015.

[10] B. Muirhead and J. R. Brophy, "Asteroid Redirect Robotic Mission Feasibility Study," presented at the Presented at teh IEEE Aerospace Conference, Big Sky, MT, 2014.

[11] D. D. Mazanek, R. G. Merrill, S. P. Belbin, D. M. Reeves, K. D. Earle, B. J. Naasz, *et al.*, "Asteroid Redirect Robotic Mission: Boulder Capture Overview Option," presented at the 50th AIAA/ASME/SAE/ASEE Joint Propulsion Conference, Cleveland, OH, 2014.

[12] N. Strange, D. Landau, T. Mcelrath, G. Lantoine, T. Lam, M. McGuire, *et al.*, "Overview of Mission Design for NASA Astreroid Redirect Robotic Mission Concept," presented at the 33rd International Electric Propulsion Conference, Washington, DC, 2013.

[13] J. H. Gilland, G. J. Williams, J. M. Burt, and J. Yim, "Carbon Back Sputter Modeling for Hall Thruster Testing," presented at the 52nd AIAA/SAE/ASEE Joint Propulsion Conference, Salt Lake City, UT, 2016.

[14] R. R. Hofer and H. Kamhawi, "Development Status of the 12.5 kW HERMeS Hall Thruster Solar Electric Propulsion Technology Demonstration Mission," presented at the 52nd AIAA/SAE/ASEE Joint Propulsion Conference, Salt Lake City, UT, 2016.

[15] W. Huang, H. Kamhawi, and T. W. Haag, "Plasma Oscillation Characterization of NASA's HERMeS Hall Thruster via High Speed Imaging," presented at the 52nd AIAA/SAE/ASEE Joint Propulsion Conference, Salt Lake City, UT, 2016.

[16] W. Huang, H. Kamhawi, and T. W. Haag, "Facility Effect Characterization Test of NASA's HERMeS Hall Thruster," presented at the 52nd AIAA/SAE/ASEE Joint Propulsion Conference, , Salt Lake City, UT, 2016.

[17] H. Kamhawi, T. W. Haag, W. Huang, D. A. Herman, G. J. Williams, P. Y. Peterson, *et al.*, "Performance, Stability, and Pressure Effects Characterization Tests of NASA's 12.5-kW Hall Effect Rocket with Magnetic Shielding (HERMeS) Thruster," presented at the 52nd AIAA/SAE/ASEE Joint Propulsion Conference, Salt Lake City, UT, 2016.

[18] T. R. Verhey, H. Kamhawi, D. M. Goebel, J. E. Polk, P. Y. Peterson, and D. A. Robinson, "Hollow Cathode Assembly Development for the HERMeS Hall Thruster," presented at the 52nd AIAA/SAE/ASEE Joint Propulsion Conference, Salt Lake City, UT, 2016.

[19] G. J. Williams, J. H. Gilland, P. Y. Peterson, H. Kamhawi, W. Huang, M. Swiatek, *et al.*, "Wear Testing of the HERMeS Thruster," presented at the 52nd AIAA/SAE/ASEE Joint Propulsion Conference, Salt Lake City, UT, 2016.

[20] T. Randolph, V. Kim, H. R. Kaufman, K. Kaufman, V. V. Zhurin, and M. Day, "Facility Effects on Stationary Plasma Thruster Testing," in *23rd International Electric Propulsion Conference*, Fort Collins, CO, USA, IEPC-093-1993.

[21] R. Hofer, P. Y. Peterson, and A. D. Gallimore, "Characterizing Vacuum Facility Backpressure Effects on the Performance of a Hall Thruster," in *27th International Electric Propulsion Conference*, Pasadena, CA, USA, IEPC-045-2001.

[22] K. D. Diamant, R. Spektor, E. J. Beiting, J. A. Young, and T. J. Curtiss, "The Effects of Background Pressure on Hall Thruster Operation," in *48th AIAA/ASME/SAE/ASEE Joint Propulsion Conference and Exhibit*, Atlanta, Georgia, USA, AIAA-3735-2012.

[23] K. D. Diamant, R. Liang, and R. L. Corey, "The Effect of Background Pressure on SPT-100 Hall Thruster Performance," in *50th AIAA/ASME/SAE/ASEE Joint Propulsion Conference and Exhibit*, Cleveland, OH, USA, AIAA-2014-3710.

[24] W. Huang, H. Kamhawi, R. B. Lobbia, and D. L. Brown, "Effect of Background Pressure on the Plasma Oscillation Characteristics of the HiVHAc Hall Thruster," in *50th AIAA/ASME/SAE/ASEE Joint Propulsion Conference and Exhibit*, Cleveland, OH, USA, AIAA-3708-2014.

[25] H. Kamhawi, W. Huang, T. Haag, and R. Spektor, "Investigation of the Effects of Facility Background Pressure on the Performance and Voltage-Current Characteristics of the High Voltage Hall Accelerator," in *50th AIAA/ASME/SAE/ASEE Joint Propulsion Conference and Exhibit*, Cleveland, OH, USA, AIAA-3707-2014.

[26] H. Kamhawi, W. Huang, T. Haag, R. Shastry, R. Thomas, J. Yim, *et al.*, "Performance and Facility Background Pressure Characterization Tests of NASA's 12.5-kW Hall Effect Rocket with Magnetic Shielding Thruster," in *34th International Electric Propulsion Conference, IEPC-2015-07*, Hyogo-Kobe, Japan, 2015.
[27] J. D. Frieman, S. T. King, M. Walker, V. Khayms, and D. King, "Role of a Conducting Vacuum Chamber in the Hall Effect Thruster Electrical Circuit," *Journal of Propulsion and Power*, vol. 30, 2014.
[28] J. A. Walker, J. D. Frieman, M. Walker, and V. Khayms, "Hall Effect Thruster Electrical Interaction with a Conductive Vacuum Chamber," in *50th AIAA/ASME/SAE/ASEE Joint Propulsion Conference and Exhibit, AIAA-2014-3711*, Cleveland, OH, USA, 2014.
[29] J. D. Frieman, S. T. King, M. Walker, V. Khayms, and D. King, "Preliminary Assessment of the Role of a Conducting Vacuum Chamber in the Hall Effect Thruster Electrical Circuit " in *50th AIAA/ASME/SAE/ASEE Joint Propulsion Conference and Exhibit, AIAA-2014-3712*, Cleveland, OH, USA, 2014.
[30] J. A. Walker, J. D. Frieman, M. Walker, V. Khayms, D. King, and P. Y. Peterson, "Electrical Facility Effects on Hall-Effect-Thruster Cathode Coupling: Discharge Oscillations and Facility Coupling," *Journal of Propulsion and Power*, 2016.
[31] J. D. Frieman, J. A. Walker, M. Walker, V. Khayms, and D. King, "Electrical Facility Effects on Hall Thruster Cathode Coupling: Performance and Plume Properties," *Journal of Propulsion and Power*, vol. 32, 2016.
[32] D. L. Brown, R. B. Lobbia, K. D. Hartley, M. Sekerak, D. King, and P. Y. Peterson, "The XR-5 and XR-5A Hall Thrusters, Part 1: Stability and Mode Transitions," in *Joint Army Navy NASA Air Force (JANNAF) conference*, Nashville, TN, 2015.
[33] M. Sekerak, D. L. Brown, R. B. Lobbia, K. D. Hartley, D. King, P. Y. Peterson, *et al.*, "The XR-5 and XR-5A Hall Thrusters, Part 2: Oscillation Behavior," in *Joint Army Navy NASA Air Force (JANNAF) conference*, Nashville, TN, 2015.
[34] R. B. Lobbia, D. L. Brown, M. Sekerak, K. D. Hartley, D. King, P. Y. Peterson, *et al.*, " The XR-5 and XR-5A Hall Thrusters, Part 3: Time-Resolved Plasma Measurements," in *Joint Army Navy NASA Air Force (JANNAF) conference*, Nashville, TN, 2015.
[35] K. D. Hartley, R. B. Lobbia, D. L. Brown, B. E. Beal, D. King, P. Y. Peterson, *et al.*, " The XR-5 & XR-5A Hall Thrusters, Part 4: Plume Properties," in *Joint Army Navy NASA Air Force (JANNAF) conference*, Nashville, TN, 2015.
[36] M. S. McDonald, "Electron Transport in Hall Thrusters," Doctorate of Philosophy, Department of Aerospace Engineering, The University of Michigan, Ann Arbor, MI, 2012.
[37] W. Huang, H. Kamhawi, R. B. Lobbia, and D. L. Brown, "Effect of Background Pressure on the Plasma Oscillation Characteristics of the HiVHAc Hall Thruster," in *50th AIAA/ASME/SAE/ASEE Joint Propulsion Conference and Exhibit, AIAA-3708-2014*, Cleveland, OH, USA, 2014.
[38] H. Kamhawi, W. Huang, T. Haag, and R. Spektor, "Investigation of the Effects of Facility Background Pressure on the Performance and Voltage-Current Characteristics of the High Voltage Hall Accelerator," in *50th AIAA/ASME/SAE/ASEE Joint Propulsion Conference and Exhibit, AIAA-3707-2014*, Cleveland, OH, USA, 2014.
[39] I. Katz, A. Lopez Ortega, D. Goebel, M. Sekerak, R. Hofer, and B. Jorns, "Performance and Facility Background Pressure Characterization Tests of NASA's 12.5-kW Hall Effect Rocket with Magnetic Shielding Thruster," in *14th Spacecraft Charging Technology Conference, ESA/ESTEC,*, Noordwijk, NL USA, 2016.
[40] R. Hofer and J. R. Anderson, "Finite Pressure Effects in Magnetically Shielded Hall Thrusters," in *50th AIAA/ASME/SAE/ASEE Joint Propulsion Conference and Exhibit, AIAA-2014-3709*, Cleveland, OH, USA, 2014.
[41] C. R. Koppel and D. Estublier, "The SMART-1 Hall Effect Thruster Around the Moon: In Flight Experience," in *29th International Electric Propulsion Conference. IEPC-2005-119*, Princeton, New Jersy, 2005.
[42] E. Y. Choueiri, "Fundamental difference between the two Hall thruster variants," *Physics of Plasmas*, vol. 8, pp. 5025-5033, Nov. 2001 2001.
[43] C. Marrese, J. E. Polk, L. B. King, A. D. Gallimore, C. Garner, S. Semenkin, *et al.*, "Analysis of Anode Layer Thruster Guard Ring Erosion," in *International Electric Propulsion Conference, IEPC-95-196*, Moscow, Russia, 1995.
[44] J. M. Sankovic, D. Manzella, and M. Osborn, "RHETT2/EPDM Development Testing," in *International Electric Propulsion Conference, IEPC-97-102*, Cleveland, OH, 1997.
[45] A. E. Solodukhin, A. V. Semenkin, S. O. Tverdohlebov, and A. V. Kochergin, "Parameters of D-80 Anode Layer Thruster in One- and Two- Stage Operation Modes," in *International Electric Propulsion Conference, IEPC-01-032*, Pasadena, Ca, 2001.
[46] D. Jacobson, "High Voltage TAL Erosion Characterization," in *Joint Propulsion Conference, AIAA-02-4257*, Indianapolis, Indiana, 2002.
[47] D. Goebel and I. Katz, *Fundamentals of Electric Propulsion: Ion and Hall Thrusters*. NJ: Wiley, Hoboken, 2008.
[48] R. R. Hofer, H. Kamhawi, I. Mikellides, D. A. Herman, J. E. Polk, W. Huang, *et al.*, "Design Methodology and Scaling of the 12.5 kW HERMeS Hall Thruster for the Solar Electric Propulsion Technology Demonstration Mission," presented at the Presented at the 62nd JANNAF Propulsion Meeting, Nashville, TN, 2015.
[49] I. Mikellides, R. R. Hofer, I. Katz, and D. M. Goebel, "Magnetic Shielding of Hall Thrusters at High Discharge Voltages," *Journal of Applied Physics*, vol. 116, 2014 2013.
[50] H. Kamhawi, D. H. Manzella, T. B. Smith, and G. R. Schmidt, "High-Power Hall Propulsion Development at NASA Glenn Research Center," presented at the Space Propulsion 2012, Bordeaux, France, 2012.

[51] I. Mikellides, I. Katz, R. Hofer, D. Goebel, K. de Grys, and A. Mathers, "Magnetic Shielding of the Acceleration Channel Walls in a Long-Life Hall Thruster," in *Joint Propulsion Conference, AIAA-10-6942*, Nashville, Tennessee 2010.
[52] J. Myers, H. Kamhawi, and J. Yim, "HERMeS Thermal Model," presented at the 51st AIAA/SAE/ASEE Joint Propulsion Conference, Orlando, FL, 2015.
[53] A. Lopez Ortega, I. Mikellides, and I. Katz, "Hall2de Numerical Simulations for the Assessment of Pole Erosion in a Magnetically-Shielded Hall Thruster," presented at the 30th International Electric Propulsion Conference, Kobe, Hyogo, Japan, 2015.
[54] H. Kamhawi, T. W. Haag, W. Huang, and R. R. Hofer, "The Voltage-Current Characteristics of the 12.5 kW Hall Effect Rocket with Magnetic Shielding at Different Background Pressure Conditions," presented at the Presented at the 62nd JANNAF Propulsion Meeting, Nashville, TN, 2015.
[55] H. Kamhawi, T. W. Haag, W. Huang, D. A. Herman, R. Thomas, R. Shastry, *et al.*, "Performance Characterization of the Solar Electric Propulsion Technology Demonstration Mission 12.5-kW Hall Thruster," presented at the 30th International Electric Propulsion Conference, Kobe, Hyogo, Japan, 2015.
[56] R. R. Hofer, H. Kamhawi, D. A. Herman, J. E. Polk, J. S. Snyder, I. Mikellides, *et al.*, "Development Approach and Status of the 12.5 kW HERMeS Hall Thruster for the Solar Electric Propulsion Technology Demonstration Mission," presented at the 30th International Electric Propulsion Conference, Kobe, Hyogo, Japan, 2015.
[57] H. Kamhawi, T. Haag, W. Huang, and R. R. Hofer, "The Voltage-Current Characteristics of the 12.5 kW Hall Effect Rocket with Magnetic Shielding at Different Background Pressure Conditions," presented at the 62nd JANNAF Propulsion Meeting, Nashville, TN, 2015.
[58] H. Kamhawi, T. Haag, W. Huang, D. A. Herman, R. Thomas, R. Shastry, *et al.*, "Performance Characterization of the Solar Electric Propulsion Technology Demonstration Mission 12.5-kW Hall Thruster," presented at the 34th International Electric Propulsion Conference, Kobe, Japan, 2015.
[59] J. Myers, H. Kamhawi, and J. Yim, "HERMeS Thermal Model," in *51st Joint Propulsion Conference*, ed. Orlando, FL, 2015.
[60] D. M. Goebel, J. E. Polk, I. G. Mikellides, and A. Lopez Ortega, "Lanthanum Hexaboride Hollow Cathode for the Asteroid Retrieval/Redirect Mission " presented at the 34th International Electric Propulsion Conference, Kobe, Japan, 2015.
[61] J. E. Polk, P. Guerrero, D. M. Goebel, I. G. Mikellides, and I. Katz, "Thermal Characteristics of Lanthanum Hexaboride Hollow Cathodes," presented at the 34th International Electric Propulsion Conference, Kobe, Japan, 2015.
[62] M. Sekerak, R. R. Hofer, J. E. Polk, B. A. Jorns, and I. G. Mikellides, "Wear Testing of a Magnetically Shielded Hall Thruster at 2000 s Specific Impulse," presented at the 34th International Electric Propulsion Conference, Kobe, Japan, 2015.
[63] R. Shastry, W. Huang, and H. Kamhawi, "Near-Surface Plasma Characterization of the 12.5-kW NASA TDU1 Hall Thruster," in *51st Joint Propulsion Conference*, ed. Orlando, FL, 2015.
[64] W. Huang, H. Kamhawi, J. Myers, J. Yim, and G. Neff, "Non-Contact Thermal Characterization of NASA's 12.5-kW Hall Thruster," in *51st Joint Propulsion Conference*, ed. Orlando, FL, 2015.
[65] G. J. Williams and H. Kamhawi, "Optical characterization of component wear and near-field plasma of the HERMeS thruster," presented at the 62nd JANNAF Propulsion Meeting, Nashville, TN, 2015.
[66] J. T. Yim and J. M. Burt, "Characterization of vacuum facility background gas through simulation and considerations for electric propulsion ground testing," in *51st Joint Propulsion Conference*, ed. Orlando, FL, 2015.
[67] R. Shastry, W. Huang, and H. Kamhawi, "Near-Surface Plasma Characterization of the 12.5-kW NASA TDU1 Hall Thruster," presented at the To be Presented at the 51st AIAA/SAE/ASEE Joint Propulsion Conference, Orlando, FL, 2015.
[68] W. Huang, H. Kamhawi, J. Myers, J. Yim, and G. Neff, "Non-Contact Thermal Characterization of NASA's 12.5-kW Hall Thruster," presented at the To be Presented at the 51st AIAA/SAE/ASEE Joint Propulsion Conference, Orlando, FL, 2015.
[69] (2016). *NASA GRC Vacuum Facility 5*. Available: https://facilities.grc.nasa.gov/epl/capabilities.html
[70] J. Yim and J. M. Burt, "Characterization of Vacuum Facility Background Gas Through Simulation and Considerations for Electric Propulsion Ground Testing," in *51st AIAA/SAE/ASEE Joint Propulsion Conference, Propulsion and Energy Forum, AIAA-2015-3825*, Orlando, FL, USA, 2015.
[71] T. W. Haag, "Thrust stand for high-power electric propulsion devices," *Review of Scientific Instruments*, vol. 62, 1991 1991.
[72] T. W. Haag and M. Osborn, "RHETT/EPDM performance characterization," in *International Electric Propulsion Conference, IEPC-97-107*, Cleveland, OH, 1997.
[73] K. G. Xu and M. L. R. Walker, "High-power, null-type, inverted pendulum thrust stand," *Review of Scientific Instruments*, vol. 80, 2009 2009.
[74] D. L. Brown and R. B. Lobbia, "Characterization of Hall Thruster Mode Transitions and Facility Interactions," in *Joint Army Navy NASA Air Force (JANNAF) conference*, Nashville, TN, 2015.
[75] J. D. Sommerville, "Hall-Effect Thruster--Cathode Coupling: The Effect of Cathode Position and Magnetic Field Topology," PhD, Department of Mechanical Engineering-Engineering Mechanics, Michigan Technological University, 2009.

[76] J. M. Fife, M. Martinez-Sanchez, and J. Szabo, "A Numerical Study of Low-Frequency Discharge Oscillations in Hall Thrusters," presented at the 33rd AIAA/ASME/SAE/ASEE Joint Propulsion Conference, AIAA-1997-3052, Seattle, WA, 1997.